Palaeogeography, Palaeoclimatology, Palaeoecology 674 (2025) 113041

Contents lists available at ScienceDirect

Palaeogeography, Palaeoclimatology, Palaeoecology

journal homepage: www.elsevier.com/locate/palaeo

High-frequency glacial climate instability during the Early Pleistocene: Insights from IODP site U1387 (Gulf of Cadiz)

Samanta Trotta [a], Monica Duque-Castaño [b,c], Teresa Rodrigues [b,c], Antje H.L. Voelker [b,c], Patrizia Maiorano [a], Barbara Balestra [d,e], José-Abel Flores [f], Agata Siniscalchi [a], Marina Addante [a], Maria Marino [a,*]

[a] Dipartimento di Scienze della Terra e Geoambientali, Università degli Studi di Bari Aldo Moro, 70125 Bari, Italy
[b] Instituto Português do Mar e da Atmosfera, Divisão de Geologia e Georecursos Marinhos, 1495-165 Alges, Portugal
[c] Centro de Ciências do Mar (CCMAR/CIMAR LA), Universidade do Algarve, Campus de Gambelas, 8005-139 Faro, Portugal
[d] American University, Department of Environmental Science, Washington, DC 20016, USA
[e] Paleobiology Department, National Museum of Natural History (NMNH), Smithsonian, Washington, DC 20560, USA
[f] Universidad de Salamanca, Departamento de Geologia, Salamanca, Spain

ARTICLE INFO

Editor: Prof. M Elliot

Keywords:
Calcareous plankton
Alkenone-SST
Benthic and planktonic $\delta^{18}O$
Millennial climate variability
North Atlantic

ABSTRACT

We provide new high-resolution data on alkenone-derived sea surface temperature (SST) and calcareous plankton key taxa in temporally well constrained, high resolution benthic and planktonic oxygen isotope records at Integrated Ocean Drilling Program site U1387 in the Gulf of Cadiz. The investigated time interval encompasses the Early Pleistocene marine isotope stages (MIS) 48 to MIS 43. The aim is to evidence millennial climate variability during glacial phases of the "41 kyr world" and understand the impact of North Atlantic climate dynamics on the southern Portuguese margin. *Neogloboquadrina pachyderma* and *Coccolithus pelagicus* ssp. *pelagicus* record prominent, short-term abundance peaks concurrent with short-term SST minima and heavier values of ™^{18}O in late MIS 48 and in the middle of MIS 46 and MIS 44. Superimposed on the obliquity and precession forcing, the wavelet analysis carried out on selected proxies (planktonic ™^{18}O, *N. pachyderma*, *C. pelagicus* ssp. *pelagicus*, alkenone derived sea surface temperature) highlighted the occurrence of a higher frequency climate variability (<7 ky) mostly in glacial time windows and recalling the millennial-scale climate oscillations known from the Middle and Late Pleistocene. These brief colder episodes in the Gulf of Cadiz were contemporary to the weakening of the Atlantic Meridional Overturning Circulation, water column stratification, and Ice Rafted Detritus (IRD) events in the IRD belt as recorded in paleoenvironmental proxies from northern Atlantic reference sites, evidencing a southward shift of the subarctic front and European icesheet instability. At site U1387, they have been interpreted as terminal stadial (in late MIS 48) and stadial events (in MIS 46 and MIS 44) indicating that the millennial-scale variability during the early Pleistocene was strong enough to affect the mid-latitudes of the southern Portuguese margin.

1. Introduction

Past suborbital-scale climate changes during the Quaternary, as also recorded along the Iberian margin, have been observed in multiple geochemical, organic, and plankton group proxy records, mostly during the Middle and Late Pleistocene (e.g., Martrat et al., 2007; Hodell et al., 2008, 2013, 2015, 2023; Incarbona et al., 2010; Pénaud et al., 2011; Penaud et al., 2016; Penaud et al., 2022; Hernández-Almeida et al., 2012; Amore et al., 2012; Marino et al., 2014; Maiorano et al., 2015; Hodell and Channell, 2016; Rodrigues et al., 2017; Argenio et al., 2021; González-Lanchas et al., 2021; Girone et al., 2023). Only a few studies at high temporal resolution have evaluated climate variability during the Early Pleistocene (e.g., Voelker et al., 2015, 2022a; Martinez-Sanchez et al., 2019; Liautaud et al., 2020; Trotta et al., 2022, 2024; Barker et al., 2022). The mid-latitude Iberian margin is a crucial area for investigating paleoclimate due to its capability to capture surface and deep-water

* Corresponding author.
E-mail address: maria.marino@uniba.it (M. Marino).

https://doi.org/10.1016/j.palaeo.2025.113041
Received 1 February 2025; Received in revised form 15 April 2025; Accepted 18 May 2025
Available online 20 May 2025

signals from both the North Atlantic and the Southern Ocean. It records the modification of the Atlantic meridional overturning circulation (AMOC) linked to climate dynamics (Shackleton et al., 2000; Hodell and Channell, 2016; Hodell et al., 2015, 2023). Recent studies (Bajo et al., 2020; Zhang et al., 2021; Barker et al., 2022) have explored the Early Pleistocene to understand the climate dynamics of the "41 kyr world" forced by the obliquity orbital parameter, and the differences with respect to the well-known "100 kyr world" when the glacial-interglacial cycles mainly responded to eccentricity (Berger and Jansen, 1994). Less expanded ice volumes characterized the "41 kyr world" (Clark et al., 2006; Elderfield et al., 2012; Rohling et al., 2014) together with the more symmetric pattern of glacial-interglacial $\delta^{18}O$ records highlighting that the climate variables responded almost linearly to orbital insolation forcing (Imbrie et al., 1992, 1993; Raymo and Nisancioglu, 2003; Maslin and Brierley, 2015; Chalk et al., 2017, 2019; Farmer et al., 2019), and explaining the lack of glacial terminations. In contrast, a "sawtooth-shaped" $\delta^{18}O$ pattern delineated the glacial cycles of the "100 kyr world", with more severe glacial and interglacial phases and increased ice volumes (Zhang et al., 2021; Barker and Knorr, 2023). An additional feature of late Pleistocene glacial phases is the occurrence of abrupt short-term climate events known as Heinrich (H) and Dansgaard-Oeschger (D—O) events. They record high amplitude temperature oscillations at millennial periodicities (see Rahmstorf, 2002 for a summary). The D—O events, marking the abrupt transition from a cold stadial to a warm interstadial, were firstly recognized in Greenland ice cores (Dansgaard et al., 1993; Bond et al., 1993) and then in many marine sediments (e.g., Voelker et al., 2002). They start in less than 30 years (Clark et al., 2002), recording a temperature increase of 5–10 °C and have a periodicity of 1–2 kyr. Each of the D—O events in Greenland are expressed in the Iberian margin planktonic $\delta^{18}O$ signal over the last glacial cycle (e.g., Shackleton et al., 2000, 2004). Heinrich events, characterized by the presence of ice-rafted debris (IRD), are cold intervals with even larger amplitude than D/O warmings (e.g., Bond et al., 1993, 1999; Cacho et al., 1999). They have a quasi-periodic recurrence at intervals between 6 and 7 kyr. Such millennial scale climate variability has been attributed to multiple complex mechanisms like solar emission variability, changes in deep-water circulation and AMOC dynamics, with important roles of freshwater fluxes from the ice melting and sea ice extension, insolation changes and variation in atmospheric CO_2 (Hodell et al., 2023, and references therein). Recently, the millennial-scale climate variability has been thought to be present not only in glacial phases of the Middle-Late Pleistocene but also during the glacial cycles of the Early Pleistocene (Raymo et al., 1998; Hodell et al., 2008, 2023; Gruetzner and Higgins, 2010; Tzedakis et al., 2015; Voelker et al., 2015, 2022a; Birner et al., 2016; Trotta et al., 2022). The increased occurrence and amplitude of millennial-scale climate variability has been considered as modulated by the 41 kyr obliquity cycle during the Early Pleistocene. It is also related to axial tilt drops below 23.5° and benthic $\delta^{18}O$ values exceeding ~3.8 ‰ (corrected to *Uvigerina* sp. level) that are indicative of a threshold response to orbital forcing (Hodell et al., 2023). Relatively rich documentation sustaining such a frame is provided by valuable proxies, but not paleontological data that are powerful tools for the recognition of paleoclimate and paleoceanographic changes and high frequency variations in the marine ecosystem.

Here we present a high-resolution study that combines calcareous nannofossil assemblages, the planktonic foraminifer *Neogloboquadrina pachyderma*, alkenone derived sea surface temperature (SST), and planktonic and benthic stable oxygen isotope records during the Early Pleistocene marine isotope stages (MIS) 48 to MIS 43 at the Integrated Ocean Drilling Program (IODP) site U1387 located south of Portugal in the Gulf of Cadiz (Fig. 1). The aim is to improve knowledge on the glacial millennial scale climate variability during the "41 kyr world". The site is in a crucial mid-latitudinal location to test the response of calcareous plankton assemblages to climate changes during a long-lasting time of the Early Pleistocene, which displayed remarkable variations related to high-latitude oceanographic and atmospheric dynamics as previously documented in shorter Early Pleistocene time intervals dynamics (Voelker et al., 2002; Trotta et al., 2022). Calcareous nannofossils are calcifying marine algae (Haptophyta) sensitive to environmental changes (Flores et al., 2000; Baumann et al., 2004) and able to record glacial-interglacial (Baumann and Freitag, 2004; Baumann et al., 2005; Flores et al., 2003; Giraudeau et al., 2004) and millennial scale climate changes (Colmenero-Hidalgo et al., 2004; Marino et al., 2008, 2014; Giraudeau et al., 2010; Amore et al., 2012; Palumbo et al., 2013a, 2013b; Maiorano et al., 2015, 2016a). In this study, we focused on the distinct abundance patterns of *Coccolithus pelagicus* ssp. *pelagicus* and *N. pachyderma* that are key cold-water taxa able to unravel short-term environmental variations in the mid-latitude North Atlantic. *Coccolithus pelagicus* ssp. *pelagicus* is a traditional subarctic taxon (McIntyre and Bé, 1967; Baumann et al., 2000; Geisen et al., 2002; Narciso et al., 2006), which dwells in cold conditions (Okada and McIntyre, 1979; Winter and Siesser, 1994). Nowadays, the planktonic foraminifer *N. pachyderma* is associated with the polar regions, and its relative abundance has been used to reveal short-term climate variation such as the recognition of H and D—O events starting from pioneering studies (Broecker et al., 1990; Bond et al., 1993, 1999). Although its dominant affinity with polar waters might have started only 1.1–1 Ma ago (Huber et al., 2000), we used the contemporaneous presence of *C. pelagicus* ssp. *pelagicus* and *N. pachyderma* combined with colder alkenone-Sea Surface Temperature ($U^{k'}_{37}$-SST) to identify abrupt cold events on the southern Portuguese margin. To highlight orbital and millennial-scale periodicities that modulated the patterns of selected environmental proxies at the site, Continuous Wavelet Transform (CWT) analysis has been performed. We compared our results with key northern Atlantic sites to evaluate mid-latitude responses to high-latitude climate dynamics.

2. Oceanographic setting

The Gulf of Cadiz, in the mid-latitudinal North Atlantic Ocean (Fig. 1A), is a crucial oceanographic area for paleoclimate reconstruction being under the influence of several Atlantic surface and deep waters and of the Atlantic-Mediterranean water exchange at surface and subsurface depth through the Gibraltar Strait. The oceanic circulation through the Gibraltar Strait consists of the westwards subsurface warm and salty Mediterranean Outflow Water (MOW, 500–1400 m) and of the relative cooler and less salty surface water masses flowing from the Atlantic Ocean into Mediterranean Sea (Machín et al., 2006; Hernández-Molina et al., 2016) (Fig. 1). The MOW (Fig. 1B) dominates the water column in the Gulf of Cadiz at intermediate depths of 500–1400 m (Ambar et al., 2002). At the surface, the Gulf of Cadiz is influenced by the eastern branch of the subtropical Azores Current (AzC, Fig. 1). The AzC and the associated Azores Front, a prominent vertical water column structure (Fasham et al., 1985), divide the North Atlantic subtropical gyre into fully subtropical waters to the south and a transitional zone of sea surface temperatures and hydrological gradient to the north (Fig. 1B). Branches of AzC flow southward forming the Canary Current (CC) (Fig. 1B). The eastern return flow of the North Atlantic subtropical gyre is the Portugal Current (PC, Fig. 1B), which slowly transports southwards cooler surface waters, partially of subpolar origin (Pérez et al., 2001; van Aken, 2001). Generally, the Azores High strengthens and shifts northward during the spring-summer seasons (April to September/October), promoting upwelling of subsurface water by the

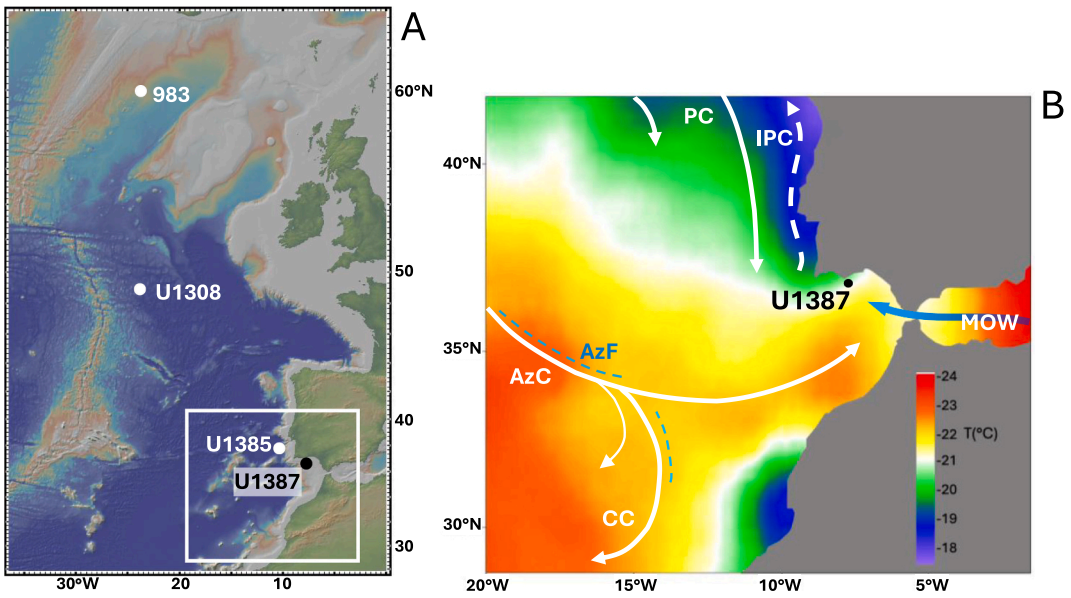

Fig. 1. A: location of IODP sites U1387, U1385 and U1308, and ODP site 983 in the North Atlantic (background map made with GeoMapApp 3.7.4). B: Mean summer sea surface temperatures (°C) at the resolution of 0.25-degree (WOA 2023; Reagan et al., 2024) in the Gulf of Cadiz, with location of site U1387 and main oceanic currents, according to Peliz et al. (2005). Background map made with Surfer 13.5. CC: Canary Current. AzC: Azores Current. PC: Portugal Current. IPC: Iberian poleward Current. MOW: Mediterranean Outflow Water.

north-easterly trade winds along the western Iberian margin (Fiúza, 1983). The dynamics of the AzC and PC form the subtropical front around 36°N (Johnson and Stevens, 2000; Peliz et al., 2005, 2007). The Iberian Poleward Current (IPC, Fig. 1B), as a branch of the AzC, consists of warm waters flowing northward mainly in autumn and winter along the slope (Frouin et al., 1990; Haynes and Barton, 1990) and is generated by the thermohaline structure of water masses and wind forcing (Peliz et al., 2003) when the Azores High weakens and moves southward causing the strengthening of south-westerly winds (Teles-Machado et al., 2016).

The climatic seasonality off the Portugal's coast is influenced by the winter atmospheric pressure gradient between the Azores High and the Iceland Low systems, which defines the North Atlantic Oscillation (NAO) that is characterized by positive and negative modes (e.g., Hurrell, 1995; Trigo et al., 2004; Hernández et al., 2020). This climatic system controls the position and the intensities of the westerly winds and the moisture transport (Lionello, 2012). Furthermore, it leads to important changes in ocean temperature and sea-ice cover in the Arctic region (Hurrell, 1995; Trigo et al., 2002). Along the Portugal coast, a positive phase of the NAO promotes a northward positioning of the westerly and northwesterly winds and storm tracks over the northern European latitudes. This pattern generates drier and cooler conditions over southern Europe, the Mediterranean Sea, and northern Africa (Pittalwala and Hameed, 1991; Hurrell, 1995). In contrast, during a negative phase of the NAO, these areas are under wetter and warmer winter conditions due to the weakening and southward position of the westerly winds (Dai et al., 1997; Rodó et al., 1997; Hurrell, 1995; Daniau et al., 2007). In the northern hemisphere, the Azores High Pressure System also controls the migration of the Intertropical Convergence Zone (ITCZ) (Hays et al., 1976; Ziegler et al., 2008; Ashkenazy et al., 2010; Trommer et al., 2011). During a negative NAO phase, the ITCZ is shifted northerly, leading to wetter conditions along the Portugal coast (Chiang et al., 2003; Broccoli et al., 2006; Stoll et al., 2007; López-Otálvaro et al., 2008; Tzedakis, 2010; Sepulcre et al., 2011). The influence of NAO on the marine ecosystem during the Early Pleistocene in the Gulf of Cadiz has been recently evidenced (Trotta et al., 2024).

3. Materials and methods

3.1. Studied core material and age model

Site U1387 was recovered in the Gulf of Cadiz (36°48.321′N, 7°43.1321′W), south of Portugal (Fig. 1), during IODP Expedition 339, in December 2011. The site is located on the middle slope at a depth of about 560 m below sea level (Fig. 1). The sedimentary succession of site U1387 was divided into four lithological units (I-IV) (Expedition 339 Scientists, 2013), for a total thickness of 870 m. The study interval is collocated in Unit I, characterized by mud with nannofossil abundance varying between 30 % and 100 % (Expedition 339 Scientists, 2013). The samples analyzed cover a continuous, 43.63 m thick sedimentary interval, between 389.29 and 440.16 c-mcd (corrected meters composite depth) (Voelker et al., 2018). They derive from the combination of the sediments of three drilled holes (Hole A, Hole B, and Hole C). In particular, the sediment samples, provided by the Bremen Core Repository, have been recovered from cores U1387A-35X, −36X, −37X and -38X, cores U1387B-34X, −35X, −36X, and cores U1387C-5R, −7R. The analysis for coccolithophore assemblages were performed at a variable spacing, (rarely every 2–5 cm and frequently every 10–25 cm). This variability granted a near constant resolution (of about 300 years) and avoided occasional occurrence of bioturbated sediments. Spacing for the planktonic and benthic foraminifera stable isotope analyses was 12–13 cm (Voelker et al., 2015, 2018), whereas the lipid biomarker and planktonic foraminifera faunal analyses were done at 24–25 cm spacing, except for the MIS 47 interval where the resolution was increased to 4–6 cm (Voelker et al., 2022a). For this study, the age model for the MIS 46 to MIS 44 interval was updated from Trotta et al. (2022) by tuning the site U1387 *Globigerina bulloides* $\delta^{18}O$ record to the high-resolution

G. bulloides $\delta^{18}O$ record of IODP site U1385 on its LR04-related chronology (Hodell et al., 2023). Tuning the planktonic foraminifera isotope record of a MOW contourite site, as site U1387, to the nearby deep ocean reference site U1385 was the strategy targeted by IODP Expedition 339 as that approach would best allow to identify potential winnowing and strongly varying sedimentation rates due to MOW current activity. Since site U1385 is located within the North Atlantic Deep Water range, its benthic $\delta^{18}O$ record can directly be correlated to the LR04 stack (Hodell et al., 2023), whereas the benthic $\delta^{18}O$ signal at site U1387 might be modified by temperature and salinity changes in the MOW. In the interval older than MIS 46, i.e., beyond the age range of Expedition 339 site U1385, the age model follows Voelker et al. (2022a) and Trotta et al. (2022), which is based on tuning to IODP site U1308 (Hodell and Channell, 2016). The studied sediments cover the time interval between 1.47 Ma and 1.35 Ma (from the late MIS 48 to the end of MIS 43), in which the sedimentation rate ranges between 21 and 96 cm/kyr.

3.2. Oxygen isotopes

The epibenthic foraminifera *Planulina ariminensis* or *Cibicidoides pachyderma* have been used to produce the epibenthic $\delta^{18}O$ record (Voelker et al., 2015; Voelker Antje et al., 2022) from 570 samples (results of 132 samples for the interval between 419.11 and 441.94 c-mcd already published; Voelker et al., 2022b). For the stable isotope analysis, 2–9 specimens of either species were collected from the fraction >250 μm, and 2–3 specimens were analyzed in the mass spectrometer. Following Voelker et al. (2015) no correction was applied when combining the $\delta^{18}O$ values of both species. For the planktonic foraminifera $\delta^{18}O$ record, 5–12 clean specimens of *G. bulloides* were selected from the fraction >250 μm and about 3–6 specimens were analyzed, depending on sample weight, in 518 samples. Analysis of some samples was repeated to confirm the isotope values. The data for the MIS 45-MIS 43 cycle are presented here for the first time, whereas the data for MIS 46 to MIS 48 was published in Voelker et al., 2022a Voelker et al., 2022b) and Trotta et al. (2022). Samples were analyzed with the Thermo Fisher Scientific 253 plus gas isotope ratio mass spectrometer with a Kiel IV automated carbonate preparation device at the MARUM research center of the University Bremen (Germany). During the period of analyses, repeatability was ±0.05–0.07 ‰ based on repeated analyses of the in-house carbonate standard (ground Solnhofen limestone). The latter was calibrated against the NBS-19 reference material.

3.3. Calcareous nannofossil sample preparation and analyses

A total of three hundred twenty-four sediment samples has been analyzed and includes the older two hundred forty samples already published in Trotta et al. (2022). Slides were prepared according to the method of Flores and Sierro (1997). This technique provides to obtain slides with coccoliths distributed homogeneously and to estimate the coccoliths abundance per gram of sediment (N) according to the formula of Flores and Sierro (1997):

$$N = n^{*}\ R^{2*}\ V^{*}r^{2*}\ g^{-1^{*}}\ v^{-1}$$

where **N** is the number of coccoliths per gram of dry sediment, n is the number of coccoliths counted in a random scanned area, **R** the radius of the Petri disk (25 mm), **V** the volume of water added to the dry sediment in the vials (10 ml), **r** the radius of the visual field used in the counting (0,1 mm), **g** the dry sediment weigh (0,1 g), **v** the volume of mixture withdrawn with the micropipette (100 μm). Thanks to this method, there is the possibility of standardizing the procedure and so to make a more reliable comparison between different samples and to prepare many slides in a brief time.

Quantitative analyses have been performed using a polarized light microscope (NIKON Eclipse LV100 POL) at 1000× magnification and the coccolith abundances have been determined by counting about 500 coccoliths for each slide. This technique allows to obtain about 99 % of probability that a taxon is detected if its real abundance in the assemblage is at least 1 % (Crow et al., 1960). Reworked coccoliths/nannoliths and lithics (>10 μm) have been counted separately during the analysis (Fig. 2). Their increase may be used as a signal for stronger erosion on land during glacial lower sea levels (Trotta et al., 2022), although reworked nannoliths have been also related to submarine MOW erosion off Gibraltar Strait (Ferreira et al., 2008).

To estimate the preservation of the assemblages, the dissolution index (DI) has been calculated according to Dittert et al. (1999) and modified by Amore et al. (2012) as small *Gephyrocapsa*/(small *Gephyrocapsa* + *Calcidiscus leptoporus*). This index compares breakable (small *Gephyrocapsa*) versus dissolution-resistant placoliths (*Calcidiscus*). High values of DI are consistent with good preservation (Fig. 2).

3.4. Remarks on key calcareous nannofossil taxa

The calcareous nannofossil taxa identified in this study followed the taxonomic criteria of Young et al. (2003, 2022) and Jordan et al. (2004). For the taxonomy of the *Gephyrocapsa* genus, reference was made to Maiorano et al. (2013) in agreement with Flores et al. (2000). Here we report on the ecological preference of the main key taxa useful for paleoclimate reconstruction. *Coccolithus pelagicus* ssp. *pelagicus*, the most abundant subspecies within *C. pelagicus* group at the location of site U1387, is used as a proxy of colder sea surface (melt)waters. It is a species considered an indicator of cold waters (McIntyre and Bé, 1967; McIntyre et al., 1970), abundant in the arctic-subarctic regions (McIntyre and Bé, 1967; Baumann et al., 2000; Geisen et al., 2002) with temperatures below 10 °C (Ziveri et al., 2004). Its presence has been linked to the occurrence of polar meltwater in the North Atlantic Ocean (Parente et al., 2004; Narciso et al., 2006; Marino et al., 2011, 2014; Amore et al., 2012) and the Mediterranean Sea (Maiorano et al., 2016b; Bazzicalupo et al., 2018; Marino et al., 2018, 2020). *Gephyrocapsa* spp. (<3μm, with open central area) are a proxy of cold waters characterized by mixing and high nutrient content (Gartner et al., 1987; Beaufort et al., 1997, 2001; Bollmann, 1997; Baumann et al., 2004; Bárcena et al., 2004; Colmenero-Hidalgo et al., 2004; Bordiga et al., 2013; Maiorano et al., 2013, 2015, 2016a, 2016b; Ausín et al., 2015). *Gephyrocapsa carribbeanica* is a warm taxon since it is more abundant during the interglacial stages at the studied site, preferring warmer surface water temperatures according to Okada and McIntyre (1977), Bollmann (1997), Bollmann et al. (1998), Flores et al. (1999), and Henriksson (2000). Large *Gephyrocapsa* (>5.5μm) are abundant during glacial stages in the studied interval, suggesting a preference for cold surface water conditions (Trotta et al., 2022). Warm water taxa group (WWT), including *Discosphaera tubifera*, *Calciosolenia* sp., *Umbilicosphaera sibogae*, *and Umbilicosphaera foliosa*, is indicative of warm and oligotrophic waters being abundant in tropical-subtropical waters (Ziveri et al., 1995, 2004; Andruleit et al., 2003; Baumann et al., 2004; Boeckel and Baumann, 2004; Saavedra-Pellitero et al., 2010). *Helicosphaera pavimentum* and *Calcidiscus leptoporus* small (<5 μm) have been also included in WWT. *Helicosphaera pavimentum* is described as a warm taxon found in tropical and subtropical areas of the Pacific Ocean and Atlantic Ocean (Okada and McIntyre, 1977; Steinmetz, 1991) and in middle Pleistocene records from the Mediterranean Sea (Marino et al., 2018, 2020; Trotta et al., 2019; Quivelli et al., 2020, 2021). *Calcidiscus leptoporus* small shows a preference for warmer waters in the studied site in agreement with previous findings in the equatorial South Atlantic (Boeckel and

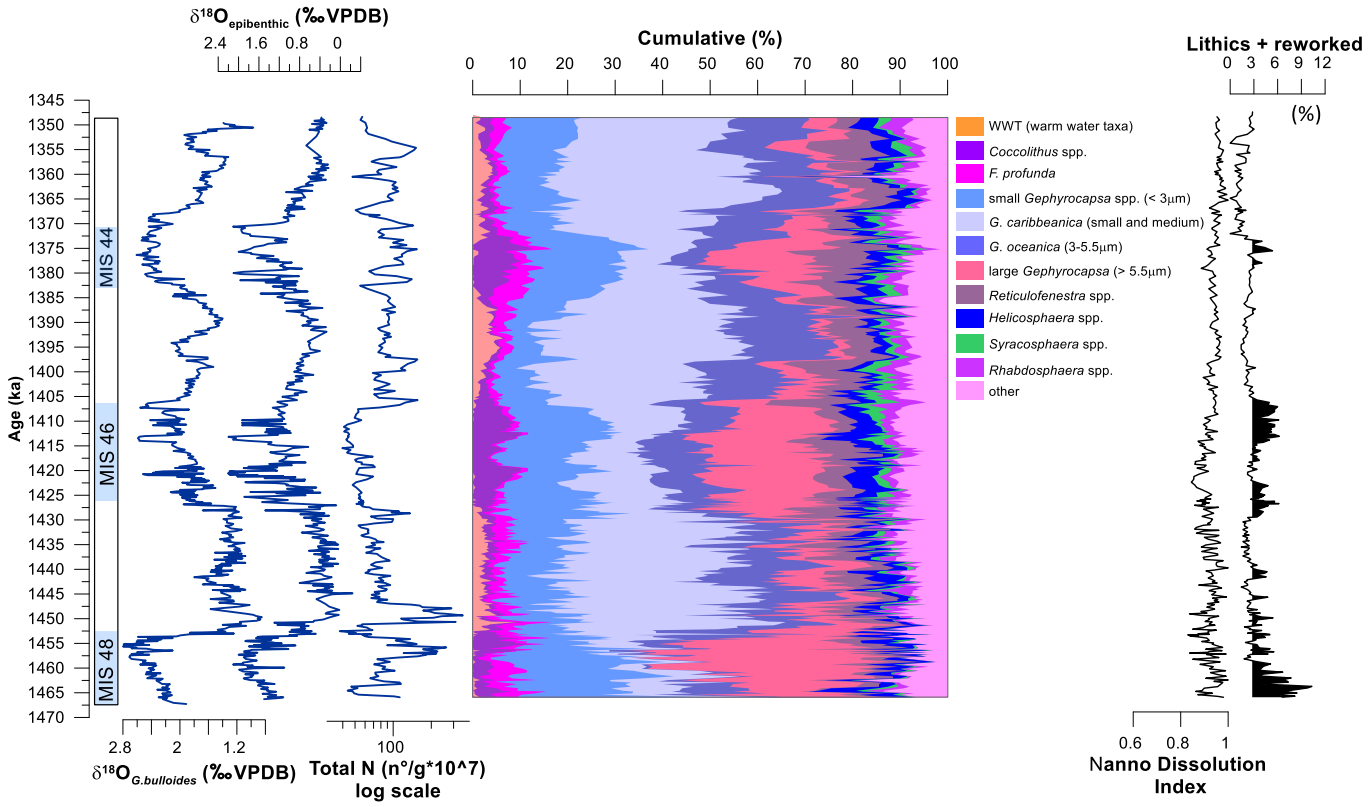

Fig. 2. IODP site U1387 records, from the left to the right: planktonic and benthic $\delta^{18}O$ (per mil VPDB), Total Nannofossil abundance (n°/g*10^7), cumulative abundance of calcareous nannofossil taxa, Nannofossil Dissolution Index, and percentages of lithics and reworked nannofossils. Glacial stages are shown on the left.

Baumann, 2008).

3.5. Planktonic foraminifera faunal analysis

The planktonic foraminifera assemblages were analyzed in 260 samples with some results (82 samples) already published in Voelker et al. (2022a). Census counts were performed in splits of the fraction >250 μm and 150–250 μm, specifically about 200 (or more) specimens were identified in the fraction >250 μm and about 100 specimens in the fraction 150–250 μm, with the aim to reach a total count of 300 or more specimens. For this study, we only used the percentage abundance of *Neogloboquadrina pachyderma* in the assemblages to identify colder surface waters incursions at the studied site.

3.6. Alkenone-based sea surface temperature

The extraction of marine lipid biomarkers was performed in a total of 255 sediment samples in the biogeochemistry lab of the Instituto Português do Mar e da Atmosfera (IPMA), following the same procedure already developed by Villanueva et al. (1997), Villanueva et al. (1997) and Rodrigues et al. (2009, 2017) to expand up to MIS 43 the record (from 1470 ka to 1408 ka, 108 sediment samples) already published in Voelker et al. (2022a). In the MIS 45 interval, lipid biomarker analyses were done in seven samples from core sections U1387C-5R-5 and U1387C-5R-6. Since those samples are outside of the revised splice sequence (Voelker et al., 2018), their depths were slightly adjusted by tuning their paleoclimatic signals to fit the ones of core U1387A-36X, thus transferring the U1387A-36X depths and ages to those U1387C-5R samples.

In this study, we used the modified alkenone unsaturation index ($U_{37}^{K'}$) based on long-chain ketones (Brassell et al., 1986; Prahl and Wakeham, 1987). To derive sea surface temperature (SST) from the $U_{37}^{K'}$ values for our site, we applied the global core-top calibration of Müller et al. (1998), which represents mean annual temperatures at the ocean surface (upper 10 m of the water column), The error for alkenone-based SST values incorporate both the calibration uncertainty (1.5 °C; Müller et al., 1998) and analytical uncertainty (~0.5 °C; Grimalt et al., 2001).

:

$$SST\left[U^{k'}_{37} = (0.033^{*}SST) + 0.044\right]$$

3.7. Multivariate statistical analyses

Multivariate statistical analyses have been carried out on the percentage abundance of nannofossil taxa to understand the environmental variables and how they affect the variations in abundance and distribution of the coccolithophores. In particular, the Principal Component Analysis (PCA) has been performed using the software PAleontology STatistic (PAST, version 4.16c) (Hammer and Harper, 2001) and the log-ratio transformation proposed by Aitchison (1981, 1986). This last method has allowed removing the constant-sum constraint (CSC) from data and to keep their true covariance structure. The PCA organizes and simplifies a series of numerical data in several variables which are called "main components" to detect the relationships between the abundances of taxa and the environmental parameters that mainly control the assemblage.

3.8. Time series analysis

A common sampling data was adopted for $\delta^{18}O_{G.\ bulloides}$, *N. pachyderma*, *C. pelagicus* ssp. *pelagicus* and alkenone-SST, and each timeseries was interpolated at 300 years that resembles the mean value for all of them. The Shape-Preserving Piecewise Cubic Interpolation was adopted (Fritsch and Carlson, 1980). Continuous Wavelet Transform

(CWT), with a Morlet wavelet function, on each series was applied to analyze the data set following Torrence and Compo (1998), and statistical significance tests were employed to evidence local regularity. Monte Carlo methods were used to assess the statistical significance against red noise backgrounds (Grinsted et al., 2004). All these procedures were carried out making a MATLAB script. To examine modulation of the time series within a chosen range of scales (period intervals) we evaluated the scale-averaged wavelet power as the weighted sum of the wavelet power spectrum over the selected range of scales. This procedure was adopted to focus on millennial oscillations.

4. Results

The results shown in the present paper include a few data published in Trotta et al. (2022) for the time interval from 1465.9 ka to 1389.9 ka (late MIS 48-MIS 45) and in Voelker et al. (2022a) for MIS 48 to MIS 47, as described in each section of Materials and Methods. Here we present extended data of planktonic and benthic foraminifera $\delta^{18}O$ records and of calcareous nannofossil assemblages, also expanding and partially improving the temporal resolution of alkenone-derived SST (Voelker et al., 2022c) and *N. pachyderma* for the long-lasting interval from ~1470 ka to 1345 ka (Figs. 2, 3). For calcareous nannofossils we show the percentage abundance of taxa and groups in a cumulative diagram to display the main taxonomic composition (Fig. 2), although here we focused on the paleoenvironmental meaning of *C. pelagicus* ssp. *pelagicus* and PC1 obtained on nannofossil assemblages (Fig. 3), referring to Trotta et al. (2022) for additional details. The studied interval, spanning MIS 48 to MIS 43 interval, encompasses into a long-lasting and poorly understood period of the Early Pleistocene, and provides deeper insights into climate and environmental changes through the integration of multiple proxies and comparisons with other North Atlantic sites (Fig. 3).

4.1. Planktonic and benthic $\delta^{18}O$

The $\delta^{18}O_{G.bulloides}$ record varies between 0.02 ‰ (minimum value) and 2.20 ‰ (maximum value) throughout the studied interval (Fig. 2). Concerning the new investigated upper interval (1389–1345 ka), the glacial MIS 44 (ca. 1370–1383 ka) records significant oscillations varying between 0.63 ‰ and 2.2 ‰. This pattern is very similar to that recorded in MIS 46, which also shows multiple high amplitude oscillations from 0.08 ‰ (1427 ka) to 2.2 ‰ (1413 ka) (Trotta et al. (2022; Voelker et al., 2022a, b). Whereas the glacial MIS 48 confirms to be a very cold and relatively more stable glacial exhibiting isotopic values almost always >1.25 ‰ with few lower points (Fig. 2). Interglacial MIS 43 records a relative stability in the planktonic $\delta^{18}O$ values ranging between 1.02 ‰ and 0.76 ‰ through 1369 ka to 1346 ka (Fig. 2). Such values are like MIS 45 and MIS 47, although the latter shows the lighter isotopic values in a plateau shape (Voelker et al., 2022a).

The $\delta^{18}O_{benthic}$ curve (Fig. 2) exhibits values between 0.85 ‰, centered at 1449.7 ka during interglacial MIS 47, and 2.68 ‰ at 1457 ka during MIS 48 (Voelker et al., 2022a, b). With respect to the pattern described by Voelker et al. (2022a) for the interval MIS 48 to early MIS 46, we may extend the observation of the outline to more glacial cycles. The influence of obliquity is recognizable in the CWT throughout the entire studied record of planktonic $\delta^{18}O$ with a confidence limit of 95 %, while the periodicity of precession is significant at 80 % in the older interval up to 1445 ka (Fig. 4). Several $\delta^{18}O$ oscillations during glacial MIS 46 and MIS 44 (Fig. 2) are recorded, particularly in planktonic $\delta^{18}O$ (Fig. 2). Three pronounced and short-term higher benthic $\delta^{18}O$ values are visible in MIS 46 centered at about 1420, 1413.4 ka, and 1497 ka (2.6 ‰). MIS 44, on the other hand, records small amplitude fluctuations in benthic $\delta^{18}O$, with values generally higher than 2.3 ‰ up to 2.61 ‰ at 1376.3 ka whereas three main heavy value peaks are detectable in planktonic $\delta^{18}O$ (Fig. 2). Millennial periodicities are significantly present mostly in glacial phases (Figs. 4, 5 a4-b4). Interglacial MIS 45 and

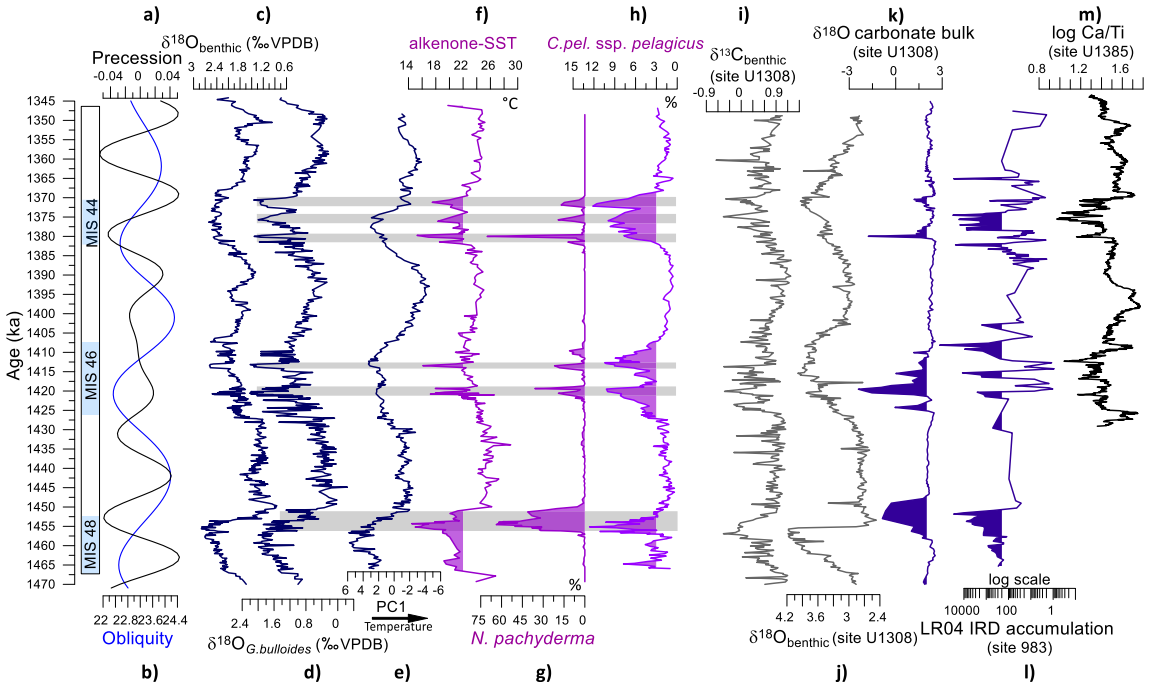

Fig. 3. Proxy data at IODP site U1387 (c to h) in relation to other IODP and ODP North Atlantic sites (i to m). a) and b) precession and obliquity (Laskar et al., 2004); c) and d) benthic and planktonic $\delta^{18}O$ records (per mil VPDB) at IODP site U1387 (Voelker et al., 2018, 2022a, b; this study); e) First Principal Component interpreted as signal of temperature of sea surface waters (this study); f) SST (°C) (Voelker et al., 2022a, 2022c, this study); g) *Neogloboquadrina pachyderma* relative abundance (inverse scale) (Voelker et al., 2022a, this study); h) *Coccolithus pelagicus* ssp. *pelagicus* relative abundance (inverse scale) (Trotta et al., 2022, this study); i) and j) benthic $\delta^{13}C$ and benthic $\delta^{18}O$ (per mil VPDB) at IODP site U1308 (Hodell and Channell, 2016); k) and l) bulk carbonate $\delta^{18}O$ (per mil VPDB) as IRD proxy at IODP site U1308 (Hodell and Channell, 2016) and IRD accumulation at ODP site 983 (inverse scale) (Barker et al., 2022); m) log Ca/Ti at IODP site U1385 (Hodell et al., 2015). Glacial stages are shown on the left. Grey bands mark stadial events.

MIS 43 appear relatively stable (mainly <1.8 ‰), although two benthic $\delta^{18}O$ increases, each lasting about 3 ka, may be seen in both, centered at about 1395 ka (2.12 ‰) and 1353 ka (1.94 ‰), respectively. The inceptions of interglacial phases of MIS 45 and MIS 43 exhibit a distinct gradual lowering of isotopic values thus differing from the more abrupt deglaciation of MIS 48/MIS 47. The $\delta^{18}O_{benthic}$ values gradually become slightly higher at the end of the two upper interglacial phases of the studied record following the value minima centered at 1389.2 ka (1.4 ‰) in MIS 45 and at 1350.5 (0.97 ‰) in MIS 43 (Fig. 2).

4.2. Calcareous nannofossil assemblages and principal component analysis

Thirty-three taxa have been identified, at the level of genus, species, subspecies and morphotypes. They are generally well preserved as revealed by the high values (0.83 to 1) for the dissolution index (Fig. 2). The total N values range from a minimum of 37.8×10^7 coccoliths/g (at 1452.5 ka) to a maximum of 355×10^7 coccoliths/g (at 1449.3 ka) (Fig. 2). The cumulative abundance of nannofossil taxa (Fig. 2) indicates that the *Gephyrocapsa* genus is the most abundant taxon in the assemblage as already determined in the MIS 48-MIS 45 interval (Trotta et al., 2022) (Fig. 2). They show percentages exceeding 85 % and include different species and morphotypes: *Gephyrocapsa* spp. < 3 μm with open central area (from 3.6 % to 35 %); large *Gephyrocapsa* > 5.5 μm (from 1.8 % to 57.2 %); *Gephyrocapsa caribbeanica* (small and medium, from 1.8 % to 49.2 %) and *Gephyrocapsa oceanica* (from 2.9 % to 27.3 %) (Fig. 2). Like in the MIS 48-MIS 45 interval (Trotta et al., 2022), the *Coccolithus pelagicus* group (*Coccolithus* spp. in Fig. 2), mostly consisting of *C. pelagicus* ssp. *pelagicus* (5–10mm) and rare and scattered *C. pelagicus* ssp. *braarudii* (>10 < 14 mm) and *C. pelagicus* ssp. *azorinus* (>14 mm), records percentage values up to 12.6 % in selected intervals corresponding with heavier planktonic $\delta^{18}O$ values (Fig. 2). The warm water taxa (WWT) group shows low percentages reaching values up to 9.2 % and clearly increases during interglacial phases (Trotta et al., 2022) (Fig. 2). *Florisphaera profunda* exhibits values up to 16.7 %, with minima of 0.4 %. *Reticulofenestra minuta* and *Reticulofenestra minutula* grouped as *Reticulofenestra* spp. in Fig. 2, reveal percentages up to 20 %. *Helicosphaera* spp. (*H. carteri*, *H. sellii*, *H. acuta*) has a maximum of 11.6 %; *Syracosphaera* spp. that include *S. histrica* and *S. pulchra*, reach up to 5.5 % (Fig. 2). *Rhabdosphaera* spp. (*R. clavigera* var. *stylifera*, *R. clavigera* var. *clavigera*) show percentages lower than 8.9 % (Fig. 2). The species with scattered occurrence and low abundance or having no clear and known ecological significance have been included in "other taxa" and are specifically: *Calcidiscus* spp. (*C. leptoporus* ssp. *leptoporus*, *C. leptoporus* ssp. *quadriperforatus*), *Ceratolithus* spp., *Pontosphaera* spp., *Pseudoemiliania lacunosa*, *Scyphosphaera* spp., *Umbilicosphaera hulburtiana*, *Brarudosphaera bigelowii*, *Pleurocrysis* sp., and holococcoliths. Cretaceous to Paleogene reworked coccoliths/nannoliths and lithic elements >10 μm exhibit abundances up to 6 % and 5.5 %, respectively, and are shown together in Fig. 2. Their low abundance did not influence the primary record of calcareous nannofossil assemblages whose composition and trend through time were not affected by MOW dynamics (Trotta et al., 2022, 2024).

The percentages of variance emerging from the PCA performed on the nannofossil assemblage are 37.42 % and 15.89 %, for the first (PC1) and second (PC2) components, respectively. Only the first principal component will be discussed here owing to its higher value and significance related to the main issue of this study, improving reconstruction of sea surface water temperature at site U1387 during the Early Pleistocene. The second component was discussed in Trotta et al. (2024). The full time series relative to the PCA is available in the Supplementary S1. The most relevant species for PC1 are indicated in bold in Table 1. Based on the higher loading values, the species that are useful to interpret the first component are: WWT group, *C. pelagicus* ssp. *pelagicus*, large *Gephyrocapsa* (> 5.5 μm), medium *G. caribbeanica*, small *G. caribbeanica* and small *Gephyrocapsa* spp. The WWT group and the small and medium *G. caribbeanica* show the most negative values, while the most positive values are represented by *C. pelagicus* ssp. *pelagicus*, large *Gephyrocapsa* and small *Gephyrocapsa* spp. Based on the ecology of the most relevant taxa for the first component, the PC1 is interpreted as a signal of temperature, with the negative values indicative of warmer sea surface waters (Fig. 3e).

4.3. Neogloboquadrina pachyderma abundance

The species shows a distribution pattern characterized by short-term abundance peaks during colder intervals (Fig. 3g). These intervals are interrupted by the total absence of the species in many samples (Fig. 3g). The first interval with higher abundances (up to 64 %) is recorded from 1456 ka to 1450 ka (MIS 48). A second interval of *N. pachyderma* high occurrences is between 1421 ka and 1410 ka, with percentage peaks varying between 11 % and 36.5 % at 1421 ka, 1419 ka, 1413 ka, and 1410 ka (Fig. 3g). Additional younger abundance peaks of the species are recorded at about 1381.5 ka, around 1380 ka (reaching a maximum of 70 %), 1376 ka, and 1372 ka, with percentages ranging in general between 12 % and 41 %.

4.4. Alkenone derived sea surface temperature

The alkenone-derived SST shows values ranging between 14.4 °C and 28.9 °C (Fig. 3). Consistently lower SST values are recorded in a short time interval centered at 1455 ka. A rapid SST increase to 26.2 °C was observed just after 1449 ka, occurring over approximately 6 kyr (Fig. 3; Voelker et al., 2022a). A continuous SST decline is recorded upward until 1422 ka with values lower than 24 °C. Immediately above, temperatures remain lower than 23 °C with short-term excursions to minimum values of 16–17.9 °C at about 1420.8 ka, 1419 ka, and 1413 ka. Afterward, temperatures start to rise to 22–24 °C until 1382 ka. Lower SST values follow upward with short-term minima of 15–18 °C centered at 1379 ka, 1376 ka, and 1371 ka. SST increases in the upper portion of the studied interval with quite stable values close to 24–25 °C. The uppermost analyzed samples record an alkenone-SST decline toward 19 °C (Fig. 3).

4.5. Time series analysis

The influence of obliquity forcing is recorded in the planktonic $\delta^{18}O$ albeit inside the cone of influence (COI) only during the central portion of the studied interval (Fig. 4). The precession is recorded (80 % significance) in the older record up to 1440 ka (Fig. 4), while millennial periodicities (<2 kyr and 5–7 kyr scale-average, Fig. 5 a4-b4) are present in glacial periods especially in MIS 46 and MIS 44. The CWT analysis of the *C. pelagicus* ssp. *pelagicus* record reveals significant (95 %) obliquity influence in the interval between 1440 ka and 1360 ka, although for the most part falls outside the COI. The precessional forcing (significant at 80 %) is recorded between 1400 ka and 1370 ka. The millennial scale periodicity (<2 kyr and 5–7 kyr scale-average) is present in all glacial intervals (Figs. 4, 5 a3-b3). The CWT analysis on the *N. pachyderma* record indicates the prominent occurrence (95 %) of millennial periodicity during glacials (Fig. 5 a2-b2), mainly in MIS 48 and MIS 44 for the 5–7 kyr and mostly in MIS 44 for <2 kyr scale-average. The obliquity influence is weak throughout the entire record and significant at 80 % in the older interval up to 1380 ka when precession influence is strong and stable until 1440 ka (Fig. 4). The CWT analysis on the alkenone-SST shows the obliquity influence throughout the studied record with higher statistical significance (95 %) from MIS 48 to the middle of MIS 44 (Fig. 4). Precession is relatively weak (80 %) from the bottom of the studied period to ca. 1440 ka (Fig. 4), while millennial periodicity is evident especially in glacial phases MIS 46 and MIS 44 for <2kyr and 5–7 kyr scale-average (Figs. 4, 5 a1-b1).

5. Discussion

5.1. Sea water condition versus calcareous plankton cold key taxa

The combined results of PC1 on calcareous nannofossil assemblages, alkenone-SST, benthic and planktonic $\delta^{18}O$, and two key cold-water taxa (*C. pelagicus* ssp. *pelagicus* and *N. pachyderma*) allow to understand major climatic shifts through time (Fig. 3). The PC1 results distinctly highlight i) glacial-interglacial cycles, ii) colder surface water conditions in late MIS 48, iii) sharp amelioration at the MIS 48-MIS 47 transition, and iv) more gradual variations through the subsequent cycle boundaries (Fig. 3e). The long-term pattern of the alkenone-SST describes glacial and interglacial variations with warmer and more stable temperatures during interglacials, generally up to 24 °C, especially in MIS 47 that appears as the warmest interglacial at site U1387 (Fig. 3f), in agreement with Voelker et al. (2022a). During glacial phases the SST decreases are outlined by two prominent minima in late MIS 48 (up to 14 °C during the MIS 48-MIS 47 deglaciation) and two and three declines in MIS 46 and MIS 44 (up to 18–15 °C), respectively, interspersed into background SST generally not higher than 21 °C, but rarely reaching 24 °C in MIS 46 and 23 °C MIS 44, and 21 °C in MIS 48. The temperature amplitudes between interglacial warmth and glacial extreme cold periods (14 °C) are very high, reaching up to 8 °C. During these glacial colder events the abundance of the planktonic foraminifer *N. pachyderma* increases up to 70 % (Fig. 3g) whereas it is generally absent during interglacials. Indeed nowadays, it is the dominant species in polar oceans (Hemleben et al., 1989; Johannessen et al., 1994; Kučera, 2007) able to live in waters with temperatures as cold as −2 °C (e.g., Darling et al., 2006; Lombard et al., 2009; Zamelczyk et al., 2021). The major, long-lasting abundance of *N. pachyderma* at the MIS 48/MIS 47 transition is related to some of the lowest alkenone-SST and higher benthic $\delta^{18}O$ values at site U1387 (Voelker et al., 2022a). This appears associated with a larger northern

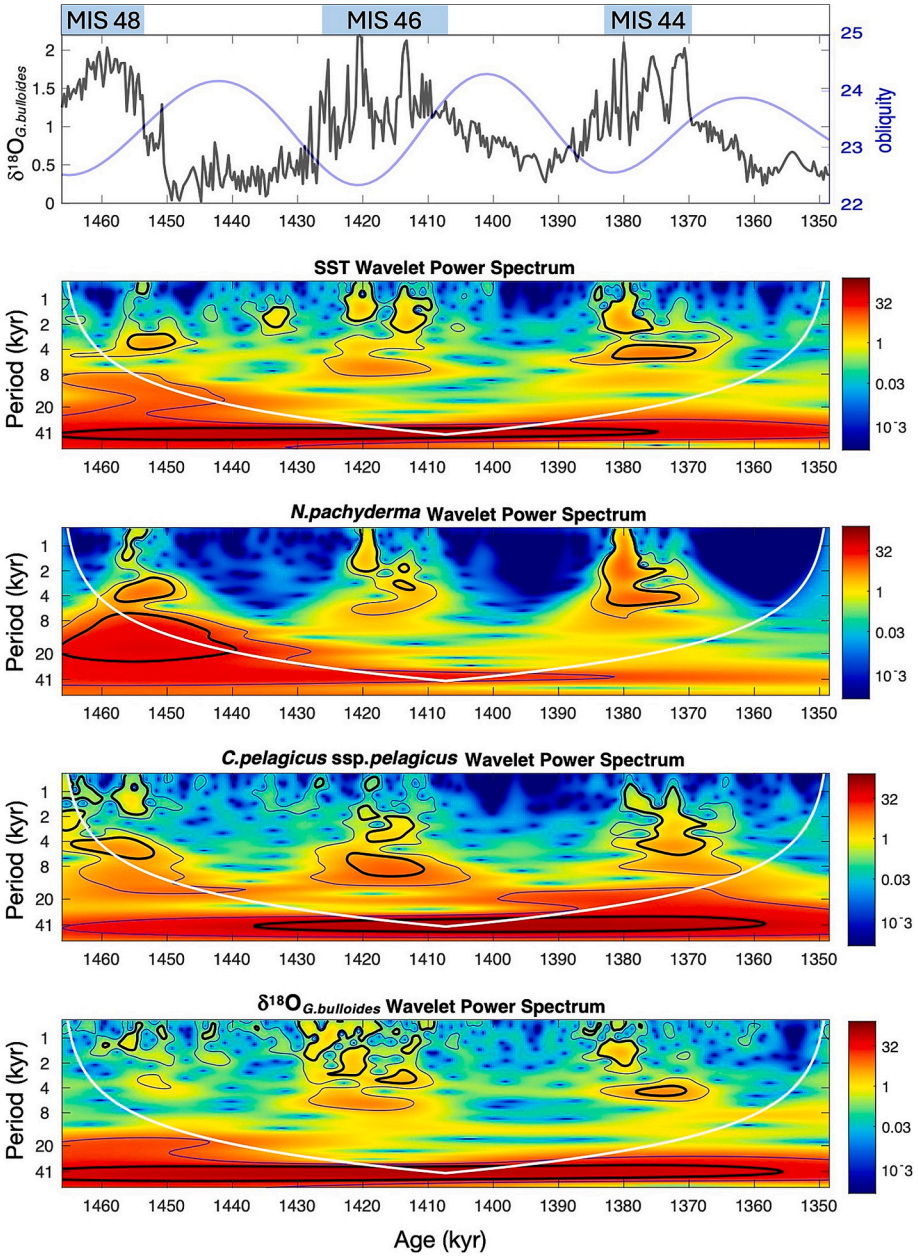

Fig. 4. Continuous Wavelet Transform (CWT) of the analyzed timeseries. The thick contour black line marks the 95 % confidence level above the red noise, while the thinner line is at 80 %. On the top is the $\delta^{18}O_{G.bulloides}$ record of IODP site U1387, together with obliquity and indication of glacials MIS 48, MIS 46 and MIS 44. (For interpretation of the references to colour in this figure legend, the reader is referred to the web version of this article.)

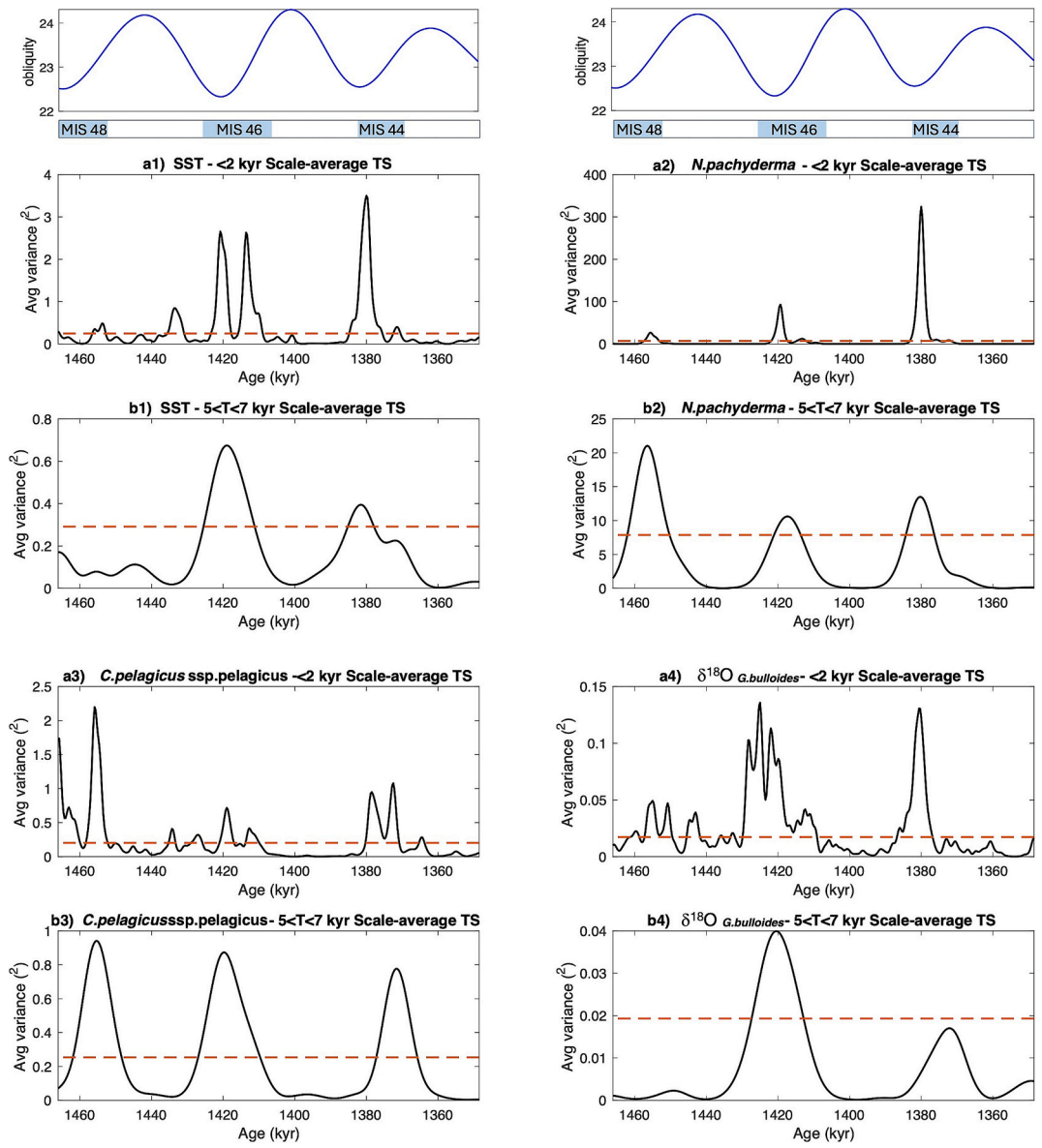

Fig. 5. Scale-averaged wavelet power in the bands lower than 2 kyr (a1-a4) and in 5–7 kyr (b1-b4) for all the four parameters. The dashed line is the 95 % confidence level in each band. Obliquity and glacials MIS 48, MIS 46 and MIS 44 are also shown on the top.

Table 1
Taxa loading of PC1 at IODP site U1387 performed on the percentages of calcareous nannofossil taxa. Higher loading values are in bold.

Taxa	PC 1
WWT	**−0.33804**
Calcidiscus spp.	0.17585
C. pelagicus* ssp. *pelagicus	**0.35989**
medium *G. caribbeanica* (3–5.5 μm)	**−0.36438**
medium *G.oceanica* (3–5.5 μm)	−0.25691
large *Gephyrocapsa* (>5.5 μm)	**0.39815**
F. profunda	0.080192
Helicosphaera spp.	0.29444
Syracosphaera spp.	−0.066213
Rhabdosphaera spp.	−0.19703
small *G. caribbeanica* (< 3 μm)	**−0.33408**
small *Gephyrocapsa* spp. (< 3 μm)	**0.34506**
Reticulofenestra minuta (< 3 μm)	−0.006891
Reticulofenestra minutula (3–5 μm)	−0.030429

hemisphere ice sheet volume as evidenced by the contemporary higher benthic $\delta^{18}O$ values recorded at the North Atlantic IODP site U1308 (Hodell and Channell, 2016) (Fig. 3j). Clear evidence of colder surface waters in the Gulf of Cadiz is supported by the abundance of *C. pelagicus* ssp. *pelagicus*, which is absent or less than 3 % in interglacial stages and noticeably increases up to 13 % during glacials (Fig. 3h), like the *N. pachyderma* pattern. The same pattern was also recorded by Parente et al. (2004) from the offshore Portugal area during the last 200 kyr. *Coccolithus pelagicus* ssp. *pelagicus* exhibits a more prolonged and continuous high abundance during glacial periods compared to *N. pachyderma*, maybe in relation to its capability to thrive in less cold temperatures. However, most peaks in abundance for the two taxa occur almost simultaneously (Fig. 3g, h), revealing a strong correspondence between phyto- and zooplankton responses to surface water temperature.

The combined records of alkenone-SST and the distribution of the key cold-water taxa indicate that they are reliable tools for paleoclimate reconstruction in the Gulf of Cadiz during the Early Pleistocene. The pronounced short-term colder events during the glacials, also evidenced by the occurrence of millennial-scale variability (Figs. 4–5), provide

additional palaeoceanographic insights into the interplay between the mid-latitude climate system and the high-latitude ice sheet melting and dynamics, as discussed below.

5.2. Millennial-scale glacial variability in the Gulf of Cadiz

The higher amplitude oscillations during glacial periods, specifically during late MIS 48, MIS 46, and MIS 44, as depicted by the $\delta^{18}O$ records (Fig. 3c-d), reflect the significant climate variability in agreement with the patterns of the alkenone-SST and of *N. pachyderma* and *C. pelagicus* ssp. *pelagicus* abundances (Fig. 3g-h). Distinct brief episodes of higher $\delta^{18}O$ values occur (Fig. 3c-d) contemporary with colder SST (Fig. 3f) and major percentage increases of the two key taxa (Fig. 3g-h). The pattern in glacial planktonic $\delta^{18}O$, markedly in MIS 46 and MIS 44, seems to recall the high frequency stadial/interstadial oscillations of Late Pleistocene glacial intervals as previously pointed out by Birner et al. (2016) and Hodell et al. (2023) for the nearby IODP site U1385. Our data from MIS 48 to MIS 43 clearly support that high frequency climate variability was experienced during the Early Pleistocene glacials, in the 41 kyr world, like during and after the Mid-Pleistocene Transition (MPT), when 100 kyr cyclicity of eccentricity dominated. Concerning the orbital periodicity, the presence of obliquity forcing throughout the studied interval is intuitive when we compare this orbital parameter with the glacial and interglacial increase and decrease of the PC1 (Fig. 3b) and $\delta^{18}O$ records (Fig. 3c-d). The CWT analyses (Fig. 4) reveal that obliquity forcing is present in the planktonic $\delta^{18}O$, alkenone-SST, and *C. pelagicus* ssp. *pelagicus* time series (Figs. 4–5), although acknowledging that the length of our time series is at the statistical limit for that cyclicity. Precession strongly modulated the *N. pachyderma* abundance pattern in the 1465–1440 kyr time window, with 95 % confidence level above the red noise. The response of this cold taxon to precession was already evidenced in Pliocene (Caruso, 2004) and Early Pleistocene (Girone et al., 2013) successions in the Mediterranean area.

Notably, superimposed on the orbital forcing, millennial-scale climate variability is evident at site U1387 (Figs. 4–5), consistent with the patterns observed in our proxies (Fig. 3d, f-h). In particular, the millennial periodicities (<2 kyr and 5–7 kyr scale-average) are significantly present, with different confidence limits (Fig. 4), during glacial cycles in all the selected proxies. Fig. 5 shows the variance versus time averaged over the scale <2 kyr and 5–7 kyr with respect to the background red noise at the same scale intervals, adding information on the importance of such periodicities throughout the studied record. A shared idea is that the occurrence of higher frequency variability is related to lower obliquity. In fact, obliquity lower than 23.5°, like during the investigated interval (Fig. 3b), combined with benthic $\delta^{18}O$ exceeding ~3.8 ‰ is thought to have favored glacial millennial variability during both the "100 kyr world" (Shackleton et al., 2000) and the "41 kyr world" (Hodell et al., 2008, 2023). Values of benthic $\delta^{18}O$ exceeding ~3.8 ‰ are recorded at North Atlantic site U1308 (Fig. 3j) highlighting the presence of (continental) ice sheets because the increased meridional heat and moisture flux to the high latitudes and reduced insolation at high latitude during obliquity lower than 23.5° led to colder temperatures and sea ice expansion (Hodell et al., 2023). Therefore, the multiple short-term oscillations during MIS 46 and MIS 44, suggestive of climate instability, may be related to the presence of continental ice sheets that however had lower volumes than during the Middle and Late Pleistocene. This agrees with Niu et al. (2019) who indicated strong millennial scale variability when ice sheet size is relatively low. Our results, in line with the millennial-scale variability already recorded during the Early Pleistocene intervals in the North Atlantic sites (Mc Intyre et al., 2001; Raymo et al., 1998; Barker et al., 2022), are in accordance with the peculiar high frequency variability indicated as a feature of the only glacial phases in the Early Pleistocene intervals along the Iberian Margin at site U1385 (Birner et al., 2016; Hodell et al., 2015, 2023). The periodicities documented by CWT analysis during the glacials at the site (Fig. 5) are likely related to AMOC dynamics and waxing and waning of unstable European ice sheets, similar to more recent Pleistocene periods.

AMOC slowdown and iceberg rafting events could have promoted cooling in the northern hemisphere even close to the latitude of site U1387 where surface waters rapidly cooled (Fig. 3f) possibly due to the arrival of cold meltwaters. The periodicities lower than 2 kyr and between 5 and 7 kyr scale-average found at the site U1387 (Fig. 5) recall those of D—O events (~1.5 kyr) and H events (~6 kyr) (Broecker et al., 1990; Bond et al., 1992; Heinrich, 1988; Maslin et al., 2001; Schulz, 2002), pointing to the occurrence of similar short-term climate episodes between the Early and the Middle-Late Pleistocene.

Concerning the millennial climate variability, additional information may be provided looking at the patterns of our proxies and particularly at the *N. pachyderma* record, aiming to display some difference between the glacial periods of the studied record. The major peak of *N. pachyderma* during the MIS 48/MIS 47 deglaciation, together with the lowest temperatures, would be an indication of the southernmost position of the polar-subpolar front in the northeastern Atlantic. Moreover, through the late MIS 48/MIS 47 transition longer-lasting, colder sea water conditions are evidenced by *N. pachyderma* and SST profiles, showing less pronounced multiple peaks with respect to what can be seen in MIS 46 and MIS 44 (Fig. 3g), consistent with the lack of distinctive multiple oscillations in $\delta^{18}O$ in late MIS 48, unlike MIS 46 and MIS 44 (Fig. 3c-d). This is because a sustained ice sheet growth through a glacial cycle, MIS 48 in our record, requires the absence of millennial scale variability (Siddall et al., 2008; Hodell et al., 2023). Supporting this is the low averaged variance of periodicity <2 kyr in *N. pachyderma* and $\delta^{18}O_{G.bulloides}$ and of 5–7 kyr scale-average, the latter significantly present in the species but not in the stable isotope records (Fig. 5 a2, b2, a4, b4). The lowering of planktonic $\delta^{18}O$ at the transition MIS 48/MIS 47 co-occurs especially with the later part of the *N. pachyderma* abundance maximum, reflecting the influence of low salinity surface waters during the precession minimum (insolation maximum) (Fig. 3d, g). All these data support the occurrence of the MIS 48 terminal stadial event that Voelker et al. (2022a) associated with ice-rafting within the IRD belt and a reduced AMOC. This agrees with the record of IRD accumulation at ODP site 983 (Fig. 3l) (Barker et al., 2022) and the low values of $\delta^{18}O$ bulk carbonate at IODP site U1308, as IRD indicator (Fig. 3k), which together proves low amplitude variations or their absence during MIS 48 relative to MIS 44 and MIS 46 (Fig. 3). The abrupt transition into MIS 47 recorded by the $\delta^{18}O$ patterns (Fig. 3c-d) and by the rapid SST rise and the cold taxa abundance decrease is remarkable in the studied record. It mimics, differently from the following deglaciations, the nature of terminations observed during the MPT, as already observed by Voelker et al. (2022a), Trotta et al. (2022) and Mega et al. (2024) at site U1387, and by Hodell and Channell (2016) in northern Atlantic sites. Such a result allows to sustain a strict connection between the northern Atlantic climate and oceanic hydrology in the Gulf of Cadiz during the Early Pleistocene. To this regard, it is worth mentioning that *N. pachyderma* and *C. pelagicus* ssp. *pelagicus* have been used as tracers for cold and low salinity surface waters marking meltwater influx into the mid latitudes of the North Atlantic and Mediterranean Sea during cold stadials and Heinrich-like or H events in the Middle and Late Pleistocene. The values of glacial alkenone-SST at site U1387 are comparable to those recorded for the MIS 48 terminal stadial event at IODP site U1313 (Naafs et al., 2013; Voelker et al., 2022a). However, they are not as low as during the mid-Pleistocene transition MIS 26, MIS 24, and MIS 22, when SSTs below 12 °C, even down to 9 °C at site U1387, were found (Bajo et al., 2020; Mega et al., 2024), or during the mid-Brunhes interval, when alkenone-SST dropped to 8 °C (e.g. Stein et al., 2009; Rodrigues et al., 2011, 2017). This would document that the Early Pleistocene MIS 48 was much colder at wider scale in the North Atlantic, whereas MIS 46 and MIS 44 were less cold than the subsequent ones in the Middle and Late Pleistocene. On the contrary, the abundance peaks of *N. pachyderma* and *C. pelagicus* ssp. *pelagicus* in all the glacial phases at site U1387 are surprisingly similar to or higher than those displayed in younger Pleistocene glacials from the North Atlantic

ocean (Parente et al., 2004; Marino et al., 2009, 2014; Alonso-Garcia et al., 2011; Amore et al., 2012; Palumbo et al., 2013a, 2013b; Emanuele et al., 2015; Cavaleiro et al., 2018; Martinez-Sanchez et al., 2019; González-Lanchas et al., 2021; Mega et al., 2024) and Mediterranean basin (Girone et al., 2013; Maiorano et al., 2013, 2015, 2023; Marino et al., 2008, 2018, 2020; Gonzalez-Lanchas et al., 2020; Quivelli et al., 2021). Although *N. pachyderma* in its modern form most likely developed only after 1.1–1 Ma (Huber et al., 2000) and a variant with less cold water affinity occurred in the region during the Early Pleistocene (Serrano and Guerra-Merchán, 2012), the distinct co-occurrence of both cold water indicator species and cold alkenone-SST indicate a southern position of the subpolar front and stadial event occurrences in the Gulf of Cadiz during MIS 46 and MIS 44, similar to the latest MIS 48. It is uncertain if this may imply that even during MIS 46 and MIS 44, like in MIS 48, the surface waters at site U1387 could have been characterized by the presence of a low salinity lid linked to ice sheet melting and iceberg discharge as evidenced by the bulk sediment $\delta^{18}O$ and IRD accumulation in the northern Atlantic sites 983 and U1308 (Fig. 1A), respectively (Fig. 3 k, l). However, this hypothesis cannot be totally ruled out. Looking at the benthic $\delta^{13}C$ pattern of North Atlantic site U1308 (Fig. 3i) (Hodell et al., 2008; Hodell and Channell, 2016) during glacial phases, several oscillations may be observed that are a signal of climate instability and episodes of sea water stratification and weakened North Atlantic Deep-Water production (Broecker, 1997; Barker et al., 2006) during the repeated negative excursions. Co-occurrence of lower North Atlantic Deep-Water production and ice-rafting events was also evidenced by Ohno et al. (2016) in the North Atlantic. Therefore, in such a paleoceanographic setting, we postulate, also supported by the millennial periodicity provided by the CWT analysis (Figs. 4–5), that the occurrence of iceberg discharge and surface waters freshening was responsible for a slowdown of the AMOC during the colder glacial events recorded at site U1387. Remarkably, the log (Ca/Ti) at site U1385 (Fig. 1A, Fig. 3m), which reflects the relative proportion between biogenic carbonate and detrital clay (Hodell et al., 2015), although limited to the upper portion of the studied time interval, shows multiple high amplitude oscillations and climate instability, and minima just during the colder short-term glacial episodes in MIS 46 and MIS 44 at site U1387, reinforcing the cold stadial event occurrence in the Gulf of Cadiz. The Ca/Ti minima during cold and dry conditions were associated with events of IRD discharge (e.g. Sun et al., 2021), and their co-occurrence with stadial events evidenced by the new data at site U1387 highlights a paleoclimate and paleoceanographic connection between the Gulf of Cadiz and the broader North Atlantic during the Early Pleistocene, even at millennial scale.

6. Concluding remarks

The high-resolution multiproxy investigation on sediments from site U1387 from MIS 48 to MIS 43 allowed to highlight the timing and mode of climate dynamics in the Gulf of Cadiz. The glacial-interglacial climate variability has been evidenced by the planktonic and benthic $\delta^{18}O$ records, $U^{k'}_{37}$-SST and calcareous plankton key taxa patterns, which also recorded short-term cold events during glacial phases. *Neogobloquadrina pachyderma* and *C. pelagicus* ssp. *pelagicus* emerged as useful tools to recognize glacial phases and millennial-scale colder events in the late MIS 48, in MIS 46 and MIS 44, like the more recent Pleistocene glacial cycles. Their prominent abundance peaks are indicative of the presence of subpolar waters coming from the northern Atlantic, which allowed the arctic taxa to thrive in the Gulf of Cadiz. In concert with the abundance peaks of these key calcareous plankton cold taxa, alkenone-SST record shows a glacial interglacial climate change, and a millennial climate variability with abrupt short-term decrease during glacials. Records of benthic and especially planktonic $\delta^{18}O$ show remarkable high amplitude oscillations and short-term heavier values during glacial cycles that are in phase with alkenone-SST minima and abundance peaks of *N. pachyderma* and *C. pelagicus* ssp. *pelagicus*. All together these proxies suggest the occurrence of stadial episodes during glacials. The terminal stadial phase during the MIS 48/MIS 47 deglaciation is distinctive throughout the studied interval being characterized by the heaviest values of benthic $\delta^{18}O$ in late MIS 48, followed by abrupt and high amplitude lowering toward the interglacial onset, and the lowest alkenone-SST together with a more persistent high abundance of *N. pachyderma*. This deglaciation looks like the pattern of terminations during the Middle and Late Pleistocene. The Continuous Wavelet Transform analyses on *N. pachyderma*, *C. pelagicus* ssp. *pelagicus,* planktonic $\delta^{18}O$, and alkenone-SST reveal, in addition to obliquity and precession forcing, millennial-scale climate variability mostly during glacials in the frequency bands <7 kyr (< 2 kyr and 5–7 kyr scale-average), that recall those of the Middle and Late Pleistocene D—O and H events. The correlation with other paleoclimate proxies from northern Atlantic sites suggests that the stadial episodes recorded in the Gulf of Cadiz are synchronous with the occurrence of AMOC slowdown, water column stratification, and IRD discharge in the IRD belt connected to European icesheet destabilization.

Supplementary data to this article can be found online at https://doi.org/10.1016/j.palaeo.2025.113041.

CRediT authorship contribution statement

Samanta Trotta: Writing – original draft, Methodology, Investigation, Formal analysis, Data curation, Conceptualization. **Monica Duque-Castaño:** Methodology, Investigation, Formal analysis, Conceptualization. **Teresa Rodrigues:** Writing – original draft, Methodology, Investigation, Funding acquisition, Formal analysis, Data curation, Conceptualization. **Antje H.L. Voelker:** Writing – original draft, Validation, Project administration, Methodology, Investigation, Formal analysis, Data curation, Conceptualization. **Patrizia Maiorano:** Visualization, Validation, Conceptualization. **Barbara Balestra:** Visualization, Validation, Conceptualization. **José-Abel Flores:** Visualization, Validation, Conceptualization. **Agata Siniscalchi:** Writing – original draft, Visualization, Methodology, Formal analysis, Conceptualization. **Marina Addante:** Formal analysis, Methodology. **Maria Marino:** Writing – review & editing, Writing – original draft, Visualization, Validation, Supervision, Resources, Project administration, Conceptualization.

Declaration of competing interest

The authors declare that they have no known competing financial interests or personal relationships that could have appeared to influence the work reported in this paper.

Acknowledgements

The authors thank the IODP Bremen Core Repository for providing samples of IODP site U1387 and two anonymous reviewers, which improved the first version of the manuscript. This research was financially supported by a Geoscience PhD scholarship (Bari University, Italy) and by a Loeblich-and-Tappan Student research grant from the Cushman Foundation in 2021 to ST., and benefitted from instrumental upgrades from "Potenziamento Strutturale PONa3_00369 dell'Università degli Studi di Bari, Laboratorio per lo Sviluppo Integrato delle Scienze e delle Tecnologie dei Materiali Avanzati e per dispositivi innovativi (SISTEMA)". Stable isotope measurements for site U1387 were funded by project MOWCADYN (PTDC/MAR-PRO/3761/2012), and the lipid biomarker analyses were financed by project WarmWorld (PTDC/CTA-GEO/29897/2017) and an ECORD research grant to ST. AV, MDC and TR acknowledge receiving Portuguese national funds from FCT - Foundation for Science and Technology through projects UIDB/04326/2020 (DOI:10.54499/UIDB/04326/2020), UIDP/04326/2020 (DOI:10.54499/UIDP/04326/2020) and LA/P/0101/2020 (DOI:10.54499/LA/P/0101/2020). MDC is financially supported by FCT through PhD

fellowship 2022.13116.BD. JAF acknowledges support from Ministerio de Ciencia, Innovación y Universidades (Spain) project PID2021-128322NB-I00.

Data availability

Data will be made available in the PANGAEA world data center.

References

Aitchison, J., 1981. A new approach to null correlations of proportions. J. Int. Assoc. Math. Geol. 13, 175–189.

Aitchison, J., 1986. The Statistical Analysis of Compositional Data. Chapman and Hall, New York, p. 416.

Alonso-Garcia, M., Sierro, F.J., Flores, J.A., 2011. Arctic front shifts in the subpolar North Atlantic during the Mid-Pleistocene (800–400 ka) and their implications for ocean circulation. Palaeogeogr. Palaeoclimatol. Palaeoecol. 311 (3–4), 268–280.

Ambar, I., Serra, N., Brogueira, M.J., Cabeçadas, G., Abrantes, F., Freitas, P., Gonçalves, C., Gonzalez, N., 2002. Physical, chemical and sedimentological aspects of the Mediterranean Outflow off Iberia. Deep-Sea Res. 49 (19), 4163–4177.

Amore, F.O., Flores, J.A., Voelker, A.H.L., Lebreiro, S.M., Palumbo, E., Sierro, F.J., 2012. A Middle Pleistocene Northeast Atlantic coccolithophore record: paleoclimatology and paleoproductivity aspects. Mar. Micropaleontol. 90–91, 44–59.

Andruleit, H., Stäger, S., Rogalla, U., Čepek, P., 2003. Living coccolithophores in the northern Arabian Sea: ecological tolerances and environmental control. Mar. Micropaleontol. 49 (1–2), 157–181.

Argenio, C., Flores, J.A., Balestra, B., Amore, F.O., 2021. Reconstructing Ocean surface dynamics over the last~ 25 kyr at "Shackleton Site" IODP-U1385. Palaeogeogr. Palaeoclimatol. Palaeoecol. 579, 110587.

Ashkenazy, Y., Eisenman, I., Gildor, H., Tziperman, E., 2010. The effect of Milankovitch variations in insolation on equatorial seasonality. J. Clim. 23 (23), 6133–6142.

Ausín, B., Flores, J.A., Sierro, F.J., Bárcena, M.A., Hernández-Almeida, I., Francés, G., Gutiérrez-Arnillas, E., Martrat, B., Grimalt, J.O., Cacho, I., 2015. Coccolithophore productivity and surface water dynamics in the Alboran Sea during the last 25 kyr. Palaeogeogr. Palaeoclimatol. Palaeoecol. 418, 126–140.

Bajo, P., Drysdale, R.N., Woodhead, J.D., Hellstrom, J.C., Hodell, D., Ferretti, P., Voelker, A.H.L., Zanchetta, G., Rodrigues, T., Wolff, E., Tyler, J., Frisia, S., Spötl, C., Fallick, A.E., 2020. Persistent influence of obliquity on ice age terminations since the middle Pleistocene transition. Science 367 (6483), 1235–1239. https://doi.org/10.1126/science.aaw1114.

Bárcena, M.A., Flores, J.A., Sierro, F.J., Pérez-Folgado, M., Fabres, J., Calafat, A., Canals, M., 2004. Planktonic response to main oceanographic changes in the Alboran Sea (Western Mediterranean) as documented in sediment traps and surface sediments. Mar. Micropaleontol. 53 (3–4), 423–445.

Barker, S., Knorr, G., 2023. A Systematic Role for Extreme Ocean-Atmosphere Oscillations in the Development of Glacial Conditions since the Mid Pleistocene transition. Paleoceanograph. Paleoclimatol. 38 (12) e2023PA004690.

Barker, A.K., Baker, J.A., Peate, D.W., 2006. Interaction of the rifting East Greenland margin with a zoned ancestral Iceland plume. Geology 34 (6), 481–484.

Barker, S., Starr, A., van der Lubbe, J., Doughty, A., Knorr, G., Conn, S., Lordsmith, S., Owen, L., Nederbragt, A., Hemming, S., Hall, I., Levay, L., Null, N., Berke, M.A., Brentegani, L., Caley, T., Cartagena-Sierra, A., Charles, C.D., Coenen, J.J., Crespin, J. G., Franzese, A.M., Gruetzner, J., Han, X., Hines, S.K.V., Jimenez Espejo, F.J., Just, J., Koutsodendris, A., Kubota, K., Lathika, N., Norris, R.D., Periera dos Santos, T., Robinson, R., Rolison, J.M., Simon, M.H., Tangunan, D., Yamane, M., Zhang, H., 2022. Persistent influence of precession on northern ice sheet variability since the early Pleistocene. Science 376, 961–967. https://doi.org/10.1126/science.abm4033.

Baumann, K.H., Freitag, T., 2004. Pleistocene fluctuations in the northern Benguela current system as revealed by coccolith assemblages. Mar. Micropaleontol. 52, 195–215.

Baumann, K.-H., Andruleit, H.A., Samtleben, C., 2000. Coccolithophores in the Nordic Seas: comparison of living communities with surface sediment assemblages. Topical Studies in Oceanography, Deep-Sea Research Part II. Ed J.D. Milliman 47 (9–11), 1743–1772.

Baumann, K.H., Böckel, B., Frenz, M., 2004. Coccolith contribution to South Atlantic carbonate sedimentation. In: Coccolithophores: From Molecular Processes to Global Impact, pp. 367–402. Berlin, Heidelberg.

Baumann, K.H., Andruleit, H., Böckel, B., Geisen, M., Kinkel, H., 2005. The significance of extant coccolithophores as indicators of ocean water masses, surface water temperature, and palaeoproductivity: a review. Paläontol. Z. 79, 93–112.

Bazzicalupo, P., Maiorano, P., Girone, A., Marino, M., Combourieu-Nebout, N., Incarbona, A., 2018. High-frequency climate fluctuations over the last deglaciation in the Alboran Sea, Western Mediterranean: evidence from calcareous plankton assemblages. Palaeogeogr. Palaeoclimatol. Palaeoecol. 506, 226–241.

Beaufort, L., Lancelot, Y., Camberlin, P., Cayre, O., Vincent, E., Bassinot, F., Labeyrie, L., 1997. Insolation cycles as a major control of equatorial Indian Ocean primary production. Science 278, 1451–1454.

Beaufort, L., de Garidel-Thoron, T., Mix, A.C., Pisias, N.G., 2001. ENSO-like forcing on oceanic primary production during the late Pleistocene. Science 293, 2440–2444.

Berger, W.H., Jansen, E., 1994. Mid-Pleistocene climate shift-the Nansen connection. Geophys. Monograph Series 85, 295–311.

Birner, B., Hodell, D.A., Tzedakis, P.C., Skinner, L.C., 2016. Similar millennial climate variability on the Iberian margin during two early Pleistocene glacials and MIS 3. Paleoceanograph. Paleoclimatol. 31 (1), 203–217. https://doi.org/10.1002/2015PA002868.

Boeckel, B., Baumann, K.H., 2004. Distribution of coccoliths in surface sediments of the south-eastern South Atlantic Ocean: ecology, preservation and carbonate contribution. Mar. Micropaleontol. 51 (3–4), 301–320.

Boeckel, B., Baumann, K.H., 2008. Vertical and lateral variations in coccolithophore community structure across the subtropical frontal zone in the South Atlantic Ocean. Mar. Micropaleontol. 67 (3–4), 255–273.

Bollmann, J., 1997. Morphology and biogeography of Gephyrocapsa coccoliths in Holocene sediments. Mar. Micropaleontol. 29 (3–4), 319–350.

Bollmann, J., Baumann, K.H., Thierstein, H.R., 1998. Global dominance of Gephyrocapsa coccoliths in the late Pleistocene: selective dissolution, evolution, or global environmental change? Paleoceanography 13 (5), 517–529.

Bond, G., Heinrich, H., Broecker, W., Labeyrie, L., McManus, J., Andrews, J., Houn, S., Jantschik, R., Clasen, S., Simet, C., Tedesco, K., Klas, M., Bonani, G., Ivi, S., 1992. Evidence for massive discharges of icebergs into the North Atlantic Ocean during the last glacial period. Nature 360 (6401), 245–249.

Bond, G., Broecker, W., Johnsen, S., McManus, J., Labeyrie, L., Jouzel, J., Bonani, G., 1993. Correlations between climate records from North Atlantic sediments and Greenland ice. Nature 365, 143–147. https://doi.org/10.1038/365143a0.

Bond, G.C., Showers, W., Elliot, M., Evans, M., Lotti, R., Hajdas, I., Bonani, G., Johnson, S., 1999. The North Atlantic's 1-2 kyr climate rhythm: relation to Heinrich events, Dansgaard/Oeschger cycles and the Little Ice Age. Geophysical Monograph-American Geophysical Union 112, 35–58.

Bordiga, M., Beaufort, L., Cobianchi, M., Lupi, C., Mancin, N., Luciani, V., Pelosi, N., Sprovieri, M., 2013. Calcareous plankton and geochemistry from the ODP site 1209B in the NW Pacific Ocean (Shatsky rise): New data to interpret calcite dissolution and paleoproductivity changes of the last 450 ka. Palaeogeogr. Palaeoclimatol. Palaeoecol. 371, 93–108.

Brassell, C., Eglinton, G., Marlowe, I.T., Pflaumann, U., Sarnthein, M., 1986. Molecular stratigraphy: a new tool for climatic assessment. Nature 320, 129–133.

Broccoli, A.J., Dahl, K.A., Stouffer, R.J., 2006. Response of the ITCZ to Northern Hemisphere cooling. Geophys. Res. Lett. 33 (1).

Broecker, W.S., 1997. Thermohaline circulation, the Achilles heel of our climate system: will man-made CO2 upset the current balance? Science 278 (5343), 1582–1588.

Broecker, W.S., Bond, G., Klas, M., Bonani, G., Wolfli, W., 1990. A salt oscillator in the glacial Atlantic? 1. The concept. Paleoceanography 5 (4), 469–477.

Cacho, I., Grimalt, J.O., Pelejero, C., Canals, M., Sierro, F.J., Flores, J.A., Shackleton, N. J., 1999. Dansgaard-Oeschger and Heinrich event imprints in the Alboran Sea paleotemperatures. Paleoceanography 14, 698–705.

Caruso, A., 2004. Climatic changes during upper Pliocene/lower Pleistocene at Capo Rossello (Sicily, Italy): Response from planktonic foraminifera approach. In: Coccioni, et al. (Eds.), Special Volume Grzybowski Foundation, vol. 9. University of London, pp. 17–36.

Cavaleiro, C., Voelker, A.H., Stoll, H., Baumann, K.H., Kulhanek, D.K., Naafs, B.D.A., Stein, R., Grützner, J., Ventura, C., Kucera, M., 2018. Insolation forcing of coccolithophore productivity in the North Atlantic during the Middle Pleistocene. Quat. Sci. Rev. 191, 318–336.

Chalk, T.B., Hain, M.P., Foster, G.L., Rohling, E.J., Sexton, P.F., Badger, M.P.S., Cherry, S. G., Hasenfratz, A.P., Haug, G.H., Jaccard, S.L., Martínez-García, A., Pälike, H., Pancost, R.D., Wilson, P.A., 2017. Causes of ice age intensification across the Mid-Pleistocene transition. Proc. Natl. Acad. Sci. USA 114, 13114–13119.

Chalk, T.B., Foster, G.L., Wilson, P.A., 2019. Dynamic storage of glacial CO_2 in the Atlantic Ocean revealed by boron [$CO3^{2-}$] and pH records. Earth Planet. Sci. Lett. 510, 1–11.

Chiang, J.C., Biasutti, M., Battisti, D.S., 2003. Sensitivity of the Atlantic intertropical convergence zone to last glacial maximum boundary conditions. Paleoceanography 18 (4).

Clark, P.U., Pisias, N.G., Stocker, T.F., Weaver, A.J., 2002. The role of the thermohaline circulation in abrupt climate change. Nature 415, 863–869.

Clark, P.U., Archer, D., Pollard, D., Blum, J.D., Rial, J.A., Brovkin, V., Mix, A.C., Pisias, N. G., Roy, M., 2006. The middle Pleistocene transition: Characteristics, mechanisms, and implications for long-term changes in atmospheric pCO_2. Quat. Sci. Rev. 25, 3150–3184.

Colmenero-Hidalgo, E., Flores, J.A., Sierro, F.J., Barcena, M.A., Lowemark, L., Schonfeld, J., Grimalt, J.O., 2004. Ocean-surface water response to short-term climate changes revealed by coccolithophores from the Gulf of Cadiz (NE Atlantic) and Alboran Sea (W Mediterranean). Palaeogeogr. Palaeoclimatol. Palaeoecol. 205 (317–336), v.

Crow, E.L., Davis, F.A., Maxfield, M.W., 1960. Statistics Manual. Dover, New York, p. 320.

Dai, A., Fung, I.Y., Del Genio, A.D., 1997. Surface observed global land precipitation variations during 1900e88. J. Clim. 10, 2943–2962.

Daniau, A.L., Sánchez-Goñi, M.F., Beaufort, L., Laggoun-Défarge, F., Loutre, M.F., Duprat, J., 2007. Dansgaard–Oeschger climatic variability revealed by fire emissions in southwestern Iberia. Quat. Sci. Rev. 26 (9–10), 1369–1383.

Dansgaard, W., Johnsen, S., Clausen, H., Dahl-Jensen, D., Gundestrup, N.S., Hammer, C. U., Hvldberg, C.S., Steffensen, J.P., Svelnbjomsdottirt, A.E., Jouzel, J., Bond, G., 1993. Evidence for general instability of past climate from a 250-kyr ice-core record. Nature 364, 218–220. https://doi.org/10.1038/364218a0.

Darling, K.F., Kucera, M., Kroon, D., Wade, C.M., 2006. A resolution for the coiling direction paradox in Neogloboquadrina pachyderma. Paleoceanography 21, PA2011.

Dittert, N., Baumann, K.H., Bickert, R., Henrich, R., Huber, R., Kinkel, H., Meggers, H., 1999. Carbonate dissolution in the deep-sea: Methods, quantification and paleoceanographic application. In: Fischer, G., Wefer, G. (Eds.), Use of Proxies in Paleoceanography: Examples from the South Atlantic. Springer, Berlin, pp. 255–284.
Elderfield, H., Ferretti, P., Greaves, M., Crowhurst, S., McCave, I.N., Hodell, D., Piotrowski, A.M., 2012. Evolution of ocean temperature and ice volume through the mid-Pleistocene climate transition. Science 337 (6095), 704–709.
Emanuele, D., Ferretti, P., Palumbo, E., Amore, F.O., 2015. Sea-surface dynamics and palaeoenvironmental changes in the North Atlantic Ocean (IODP Site U1313) during Marine Isotope Stage 19 inferred from coccolithophore assemblages. Palaeogeogr. Palaeoclimatol. Palaeoecol. 430, 104–117.
Site U1387. In: Expedition 339 Scientists, Stow, D.A.V., Hernández-Molina, F.J., Alvarez Zarikian, C.A., the Expedition 339 Scientists (Eds.), 2013. Proceedings IODP Exp. 339 - Mediterranean Outflow. Integrated Ocean Drilling Program Management International, Inc., Tokyo. https://doi.org/10.2204/iodp.proc.339.105.2013.
Farmer, J.R., Honisch, B., Haynes, L.L., Kroon, D., Jung, S., Ford, H.L., Raymo, M.E., Jaume-Segui, M., Bell, D.B., Goldstein, S.L., Pena, L.D., 2019. Deep Atlantic Ocean carbon storage and the rise of 100,000-year glacial cycles. Nat. Geosci. 12, 355–360.
Fasham, M.J.R., Platt, T., Irwin, B., Jones, K., 1985. Factors affecting the spatial pattern of the deep chlorophyll maximum in the region of the Azores front. Prog. Oceanogr. 14, 129–165.
Ferreira, J., Cachão, M., González, R., 2008. Reworked calcareous nannofossils as ocean dynamic tracers: the Guadiana shelf case study (SW Iberia). Estuar. Coast. Shelf Sci. 79 (1), 59–70. https://doi.org/10.1016/j.ecss.2008.03.012.
Fiúza, A.F.G., 1983. Upwelling patterns off Portugal. In: Suess, E., Thiede, J. (Eds.), Coastal Upwelling its Sediment Record. NATO Conference Series, vol 10B. Springer, Boston, MA. https://doi.org/10.1007/978-1-4615-6651-9_5.
Flores, J.A., Sierro, F.J., 1997. Revised technique for calculation of calcareous nannofossil accumulation rates. Micropaleontology 43, 321–324.
Flores, J.A., Gersonde, R., Sierro, F.J., 1999. Pleistocene fluctuations in the Agulhas Current Retroflection based on the calcareous plankton record. Mar. Micropaleontol. 37 (1), 1–22.
Flores, J.A., Bárcena, M.A., Sierro, F.J., 2000. Ocean-surface and wind dynamics in the Atlantic Ocean off Northwest Africa during the last 140 000 years. Palaeogeogr. Palaeoclimatol. Palaeoecol. 161 (3–4), 459–478.
Flores, J.A., Marino, M., Sierro, F.J., Hodell, D.A., Charles, C.D., 2003. Calcareous plankton dissolution pattern and coccolithophore assemblages during the last 600 kyr at ODP Site 1089 (Cape Basin, South Atlantic): paleoceanographic implications. Palaeogeogr. Palaeoclimatol. Palaeoecol. 196 (3–4), 409–426.
Fritsch, F.N., Carlson, R.E., 1980. Monotone Piecewise Cubic Interpolation. SIAM J. Numer. Anal. 17, 238–246.
Frouin, R., Fiúza, A.F., Ambar, I., Boyd, T.J., 1990. Observations of a poleward surface current off the coasts of Portugal and Spain during winter. J. Geophys. Res. Oceans 95 (C1), 679–691.
Gartner, S., Chow, J. Stanton, Jr, R.J., 1987. Late Neogene paleoceanography of the eastern Caribbean, the Gulf of Mexico, and the eastern equatorial Pacific. Mar. Micropaleontol. 12, 255–304.
Geisen, M., Billard, C., Broerse, A.T., Cros, L., Probert, I., Young, J.R., 2002. Life-cycle associations involving pairs of holococcolithophorid species: intraspecific variation or cryptic speciation? Eur. J. Phycol. 37 (4), 531–550.
Giraudeau, J., Jennings, A.E., Andrews, J.T., 2004. Timing and mechanisms of surface and intermediate water circulation changes in the Nordic Seas over the last 10,000 cal years: a view from the North Iceland shelf. Quat. Sci. Rev. 23 (20–22), 2127–2139.
Giraudeau, J., Grelaud, M., Solignac, S., Andrews, J.T., Moros, M., Jansen, E., 2010. Millennial-scale variability in Atlantic water advection to the Nordic Seas derived from Holocene coccolith concentration records. Quat. Sci. Rev. 29 (9–10), 1276–1287.
Girone, A., Maiorano, P., Marino, M., Kucera, M., 2013. Calcareous plankton response to orbital and millennial-scale climate changes across the Middle Pleistocene in the western Mediterranean. Palaeogeogr. Palaeoclimatol. Palaeoecol. 392, 105–116.
Girone, A., De Astis, A., Sierro, F.J., Hernández-Almeida, I., Garcia, M.A., Goñi, M.F.S., Maiorano, P., Marino, M., Trotta, S., Hodell, D., 2023. Planktonic foraminifera response to orbital and millennial-scale climate variability at the southern Iberian margin (IODP Site U1385) during Marine Isotope Stages 20 and 19. Palaeogeogr. Palaeoclimatol. Palaeoecol. 615, 111450.
Gonzalez-Lanchas, A., Flores, J.-A., Sierro, F.J., Barcena, M.A., Rigual-Hernandez, A.S., Oliveira, D., Azibeiro, L.A., Marino, M., Maiorano, P., Cortina, A., Cacho, I., Grimalt, J.O., 2020. A new perspective of the Alboran upwelling system reconstruction during the Marine Isotope Stage 11: a high-resolution coccolithophore record. Quat. Sci. Rev. 245, 106520. https://doi.org/10.1016/j.quascirev.2020.106520.
González-Lanchas, A., Flores, J.-A., Sierro, F.J., Sánchez Goñi, M.F., Rodrigues, T., Ausín, B., Oliveira, D., Naughton, F., Marino, M., Maiorano, P., Balestra, B., 2021. Control Mechanisms of primary Productivity Revealed by Calcareous Nannoplankton from Marine Isotope Stages 12 to 9 at the Shackleton Site (IODP Site U1385). Paleoceanogr. Paleoclimatol. 36. https://doi.org/10.1029/2021PA004246 e2021PA004246.
Grimalt, J.O., Calvo, E., Pelejero, C., 2001. Sea surface paleotemperature errors in U37 K′ estimation due to alkenone measurements near the limit of detection. Paleoceanography 16 (2), 226–232. https://doi.org/10.1029/1999PA000440.
Grinsted, A., Moore, J.C., Jevrejeva, S., 2004. Application of the cross wavelet transform and wavelet coherence to geophysical time series. Nonlin. Processes Geophys. 11, 561–566. https://doi.org/10.5194/npg-11-561-2004.
Gruetzner, J., Higgins, S.M., 2010. Threshold behavior of millennial scale variability in deep water hydrography inferred from a 1.1 Ma long record of sediment provenance at the southern Gardar Drift. Paleoceanography 25 (4).
Hammer, Ø., Harper, D.A., 2001. Past: paleontological statistics software package for educaton and data anlysis. Palaeontol. Electron. 4 (1), 1.
Haynes, R., Barton, E.D., 1990. A poleward flow along the Atlantic coast of the Iberian Peninsula. J. Geophys. Res. Oceans 95 (C7), 11425–11441.
Hays, J.D., Imbrie, J., Shackleton, N.J., 1976. Variations in the Earth's Orbit: Pacemaker of the Ice Ages: for 500,000 years, major climatic changes have followed variations in obliquity and precession. Science 194 (4270), 1121–1132.
Heinrich, H., 1988. Origin and consequences of cyclic ice rafting in the Northeast Atlantic Ocean during the past 130,000 years. Quat. Res. 29 (2), 142–152.
Hemleben, C., Spindler, M., Anderson, O.R., 1989. Taxonomy and Species Features. Springer-Verlag, New York, Modern planktonic foraminifera, p. 363.
Henriksson, A.S., 2000. Coccolithophore response to oceanographic changes in the equatorial Atlantic during the last 200,000 years. Palaeogeogr. Palaeoclimatol. Palaeoecol. 156 (1–2), 161–173.
Hernández, A., Cachão, M., Sousa, P., Trigo, R.M., Luterbacher, J., Vaquero, J.M., Freitas, M.C., 2020. External forcing mechanisms controlling the North Atlantic coastal upwelling regime during the mid-Holocene. Geology 49 (4), 433–437. https://doi.org/10.1130/G48112.1.
Hernández-Almeida, I., Sierro, F.J., Cacho, I., Flores, J.A., 2012. Impact of suborbital climate changes in the North Atlantic on ice sheet dynamics at the Mid-Pleistocene transition. Paleoceanography 27 (3).
Hernández-Molina, F.J., Sierro, F.J., Llave, E., Roque, C., Stow, D.A.V., Williams, T., Lofi, J., Van der Schee, M., Arnáiz, A., Ledesma, S., Rosales, C., 2016. Evolution of the gulf of Cadiz margin and Southwest Portugal contourite depositional system: Tectonic, sedimentary and paleoceanographic implications from IODP expedition 339. Mar. Geol. 377, 7–39.
Hodell, D.A., Channell, J.E.T., 2016. Mode transitions in Northern Hemisphere glaciation: co-evolution of millennial and orbital variability in Quaternary climate. Clim. Past 12 (9), 1805–1828. https://doi.org/10.5194/cp-12-1805-2016.
Hodell, D.A., Channell, J.E.T., Curtis, J.H., Romero, O.E., Röhl, U., 2008. Onset of "Hudson Strait" Heinrich events in the eastern North Atlantic at the end of the middle Pleistocene transition (~640 ka)? Paleoceanograph. Paleoclimatol. 23(4): PA4218. https://doi.org/10.1029/2008PA001591.
Hodell, D., Crowhurst, S., Skinner, L., Tzedakis, P.C., Margari, V., Channell, J.E.T., Kamenov, G., Maclachlan, S., Rothwell, G., 2013. Response of Iberian margin sediments to orbital and suborbital forcing over the past 420 ka. Paleoceanograph. Paleoclimatol. 28 (1), 185–199. https://doi.org/10.1002/palo.20017.
Hodell, D., Lourens, L., Crowhurst, S., Konijnendijk, T., Tjallingii, R., Jiménez-Espejo, F., Skinner, L., Tzedakis, P.C., Abrantes, F., Acton, G.D., et al., 2015. A reference time scale for Site U1385 (Shackleton Site) on the SW Iberian margin. Glob. Planet. Chang. 133, 49–64.
Hodell, D.A., Crowhurst, S.J., Lourens, L., Margari, V., Nicolson, J., Rolfe, J.E., Skinner, L.C., Thomas, N.C., Tzedakis, P.C., Mleneck-Vautravers, M.J., Wolff, E.W., 2023. A 1.5-million-year record of orbital and millennial climate variability in the North Atlantic. Clim. Past 19 (3), 607–636. https://doi.org/10.5194/cp-19-607-2023.
Huber, R., Meggers, H., Baumann, K.H., Raymo, M.E., Henrich, R., 2000. Shell size variation of the planktonic foraminifer Neogloboquadrina pachyderma sin. In the Norwegian-Greenland Sea during the last 1.3 Myrs: implications for paleoceanographic reconstructions. Palaeogeogr. Palaeoclimatol. Palaeoecol. 160 (3–4), 193–212. https://doi.org/10.1016/S0031-0182(00)00066-3.
Hurrell, J.W., 1995. Decadal trends in the North Atlantic Oscillation: regional temperatures and precipitation. Science 269, 676–679.
Imbrie, J., Boyle, E., Clemens, S., Duffy, A., Howard, W., Kukla, G., Kutzbach, J., Martinson, D., McIntyre, A., Mix, A., Molfino, B., Morley, J., Peterson, L., Pisias, N., Prell, W., Raymo, M., Shackleton, N., Toggweiler, J., 1992. On the structure and origin of major glaciation cycles, 1, Linear responses to Milankovitch forcing. Paleoceanography 7 (6), 701–738. https://doi.org/10.1029/92PA02253.
Imbrie, J., Berger, A., Boyle, E.A., Clemens, S.C., Duffy, A., Howard, W.R., Kukla, G., Kutzbach, J., Martinson, D.G., McIntyre, A., Mix, A.C., Molfino, B., Morley, J.J., Peterson, L.C., Pisias, N.G., Prell, W.L., Raymo, M.E., Shackleton, N.J., Toggweiler, J. R., 1993. On the structure and origin of major glaciation cycles 2. The 100.000-year cycle. Paleoceanography 8, 699–735. https://doi.org/10.1029/93PA02751.
Incarbona, A., Martrat, B., Di Stefano, E., Grimalt, J.O., Pelosi, N., Patti, B., Tranchida, G., 2010. Primary productivity variability on the Atlantic Iberian margin over the last 70,000 years: evidence from coccolithophores and fossil organic compounds. Paleoceanography 25 (2), PA2218. https://doi.org/10.1029/2008PA001709.
Johannessen, T., Jansen, E., Flatøy, A., Ravelo, A.C., 1994. The relationship between surface water masses, oceanographic fronts and paleoclimatic proxies in surface sediments of the Greenland, Iceland, Norwegian Seas. In: Carbon Cycling in the Glacial Ocean: Constraints on the Ocean's Role in Global Change: Quantitative Approaches in Paleoceanography. Springer, Berlin Heidelberg, pp. 61–85.
Johnson, J., Stevens, I., 2000. A fine resolution model of the eastern North Atlantic between the Azores, the Canary Islands and the Gibraltar Strait. Deep-Sea Res. I Oceanogr. Res. Pap. 47 (5), 875–899.
Jordan, W.R., Cros, L., Young, R.J., 2004. A revised classification scheme for living Haptophytes. Micropaleontology 50, 55–79.
Kučera, M., 2007. Chapter Six Planktonic Foraminifera as Tracers of Past Oceanic Environments, in Developments in Marine Geology. Elsevier, pp. 213–262. https://doi.org/10.1016/S1572-5480(07)01011-1.

Laskar, J., Robutel, P., Joutel, F., Gastineau, M., Correia, A.C., Levrard, B., 2004. A long-term numerical solution for the insolation quantities of the Earth. Astron. Astrophys. 428 (1), 261–285.
Liautaud, P.R., Hodell, D.A., Huybers, P.J., 2020. Detection of significant climatic precession variability in early Pleistocene glacial cycles. Earth Planet. Sci. Lett. 536, 116137.
Lionello, P., 2012. The climate of the Mediterranean region, from the past to the future. Elsevier. https://doi.org/10.1016/C2011-0-06210-5.
Lombard, F., Labeyrie, L., Michel, E., Spero, H.J., Lea, D.W., 2009. Modelling the temperature dependent growth rates of planktic foraminifera. Mar. Micropaleontol. 70 (1–2), 1–7.
López-Otálvaro, G., Flores, J., Sierro, F.J., Cacho, I., Grimalt, J.O., Michel, E., Cortijo, E., Labeyrie, L.D., 2008. Late Pleistocene paleoproductivity patterns during the last climatic cycle in the Guyana Basin as revealed by calcareous nannoplankton. Earth 3, 11–40.
Machín, F., Pelegrí, J.L., Marrero-Díaz, A., Laiz, I., Ratsimandresey, A.W., 2006. Near-surface circulation in the southern Gulf of Cádiz. Deep-Sea Res. II Top. Stud. Oceanogr. 53 (11−13), 1161–1181.
Maiorano, P., Tarantino, F., Marino, M., De Lange, G.J., 2013. Paleoenvironmental conditions at Core KC01B (Ionian Sea) through MIS 13–9: evidence from calcareous nannofossil assemblages. Quat. Int. 288, 97–111.
Maiorano, P., Marino, M., Balestra, B., Flores, J.A., Hodell, D.A., Rodrigues, T., 2015. Coccolithophore variability from the Shackleton Site (IODP Site U1385) through MIS 16-10. Glob. Planet. Chang. 133, 35–48.
Maiorano, P., Girone, A., Marino, M., Kucera, M., Pelosi, N., 2016a. Sea surface water variability during the Mid-Brunhes inferred from calcareous plankton in the western Mediterranean (ODP Site 975). Palaeogeogr. Palaeoclimatol. Palaeoecol. 459, 229–248.
Maiorano, P., Bertini, A., Capolongo, D., Eramo, G., Gallicchio, S., Girone, A., Pinto, D., Ventruti, G., Marino, M., 2016b. Climate signatures through marine isotope stage 19 in the Montalbano Jonico section (southern Italy): a land-sea perspective. Palaeogeogr. Palaeoclimatol. Palaeoecol. 461, 341–361.
Maiorano, P., Flores, J.A., Marino, M., Ducassou, E., Trotta, S., Balestra, B., 2023. Surface water dynamics of the last 20 kyr documented by coccolithophores in the Gulf of Cadiz. Palaeogeogr. Palaeoclimatol. Palaeoecol. 617, 111498.
Marino, M., Maiorano, P., Lirer, F., 2008. Changes in calcareous nannofossil assemblages during the Mid-Pleistocene Revolution. Mar. Micropaleontol. 69 (1), 70–90.
Marino, M., Maiorano, P., Lirer, F., Pelosi, N., 2009. Response of calcareous nannofossil assemblages to paleoenvironmental changes through the mid-Pleistocene revolution at Site 1090 (Southern Ocean). Palaeogeogr. Palaeoclimatol. Palaeoecol. 280 (3–4), 333–349.
Marino, M., Maiorano, P., Flower, B.P., 2011. Calcareous nannofossil changes during the Mid-Pleistocene Revolution: Paleoecologic and paleoceanographic evidence from North Atlantic Site 980/981. Palaeogeogr. Palaeoclimatol. Palaeoecol. 306 (1–2), 58–69.
Marino, M., Maiorano, P., Tarantino, F., Voelker, A., Capotondi, L., Girone, A., Lirer, F., Flores, J.-A., Naafs, B.D.A., 2014. Coccolithophores as proxy of sea-water changes at orbital-to-millennial scale during middle Pleistocene Marine Isotope Stages 14-9 in North Atlantic core MD01-2446. Paleoceanography 29, 518–532.
Marino, M., Girone, A., Maiorano, P., Di Renzo, R., Piscitelli, A., Flores, J.A., 2018. Calcareous plankton and the mid-Brunhes climate variability in the Alboran Sea (ODP Site 977). Palaeogeogr. Palaeoclimatol. Palaeoecol. 508, 91–106.
Marino, M., Girone, A., Gallicchio, S., Herbert, T., Addante, M., Bazzicalupo, P., Quivelli, O., Bassinot, F., Bertini, A., Nomade, N., Ciaranfi, N., Maiorano, P., 2020. Climate variability during MIS 20–18 as recorded by alkenone-SST and calcareous plankton in the Ionian Basin (Central Mediterranean). Palaeogeogr. Palaeoclimatol. Palaeoecol. 560, 110027.
Martinez-Sanchez, M., Flores, J.A., Palumbo, E., Alonso-Garcia, M., Sierro, F.J., Amore, F.O., 2019. Reconstruction of surface water dynamics in the North Atlantic during the Mid-Pleistocene (~ 540–400 ka), as inferred from coccolithophores and planktonic foraminifera. Mar. Micropaleontol. 152, 101730.
Martrat, B., Grimalt, J.O., Shackleton, N.J., Abreu, L.d., Hutterli, M.A., Stocker, T.F., 2007. Four climate cycles of recurring deep and surface water destabilizations on the Iberian margin. Science 317 (5837), 502–507. https://doi.org/10.1126/science.1139994.
Maslin, M.A., Brierley, C.M., 2015. The role of orbital forcing in the early Middle Pleistocene transition. Quat. Int. 389, 47–55.
Maslin, M., Seidov, D., Lowe, J., 2001. Synthesis of the Nature and Causes of Rapid climate Transitions during the Quarternary. In: Seidov, D.B., Haupt, J., Maslin, M. (Eds.), the Oceans and Rapid climate Change. https://doi.org/10.1029/GM126p0009.
Mc Intyre, K., Delaney, M.L., Ravelo, A.C., 2001. Millennial-scale climate change and oceanic processes in the late Pliocene and early Pleistocene. Paleoceanography 16 (5), 535–543.
McIntyre, A., Bé, A.W., 1967. Modern coccolithophoridae of the Atlantic Ocean—I. Placoliths and cyrtoliths. In: Deep Sea Research and Oceanographic Abstracts, vol. 14(5). Elsevier, pp. 561–597.
McIntyre, A., Bé, A.W., Roche, M.B., 1970. Modern Pacific Coccolithophorida: a paleontological thermometer. Trans. N. Y. Acad. Sci. 32 (6 Series II), 720–731.
Mega, A.M., Rodrigues, T., Salgueiro, E., Padilha, M., Kuhnert, H., Voelker, A.H.L., 2024. Subtropical gyre persistence in the Gulf of Cadiz, southern Iberian margin, interrupted by extremely cold surface water incursions during the Early–Middle Pleistocene transition. EGUsphere [preprint]. https://doi.org/10.5194/egusphere-2024-3185.
Müller, P.J., Kirst, G., Ruhland, G., Von Storch, I., Rosell-Melé, A., 1998. Calibration of the alkenone paleotemperature index U37K′ based on core-tops from the eastern South Atlantic and the global ocean (60 N-60 S). Geochim. Cosmochim. Acta 62 (10), 1757–1772.
Naafs, B.D.A., Hefter, J., Stein, R., 2013. Millennial-scale ice rafting events and Hudson Strait Heinrich (−like) events during the late Pliocene and Pleistocene: a review. Quat. Sci. Rev. 80, 1–28.
Narciso, A., Cachao, M., De Abreu, L., 2006. *Coccolithus pelagicus* subsp. pelagicus versus *Coccolithus pelagicus* subsp. braarudii (Coccolithophore, Haptophyta): A proxy for surface subarctic Atlantic waters off Iberia during the last 200 kyr. Mar. Micropaleontol. 59 (1), 15–34. https://doi.org/10.1016/j.marmicro.2005.12.001.
Niu, L., Lohmann, G., Gowan, E.J., 2019. Climate noise influences ice sheet mean state. Geophys. Res. Lett. 46 (16), 9690–9699.
Ohno, M., Hayashi, T., Sato, M., Kuwahara, Y., Mizuta, A., Kita, I., Sato, T., Kano, A., 2016. Millennial-scale interaction between ice sheets and ocean circulation during marine isotope stage 100. Front. Earth Sci. 4, 55.
Okada, H., McIntyre, A., 1977. Modern coccolithophores of the Pacific and North Atlantic oceans. Micropaleontology 23 (1), 1–55. https://doi.org/10.2307/1485309.
Okada, H., McIntyre, A., 1979. Seasonal distribution of modern coccolithophores in the western North Atlantic Ocean. Mar. Biol. 54, 319–328.
Palumbo, E., Flores, J.A., Perugia, C., Petrillo, Z., Voelker, A.H.L., Amore, F.O., 2013a. Millennial scale coccolithophore paleoproductivity and surface water changes between 445 and 360 ka (Marine Isotope Stages 12/11) in the Northeast Atlantic. Palaeogeogr. Palaeoclimatol. Palaeoecol. 383, 27–41.
Palumbo, E., Flores, J.A., Perugia, C., Emanuele, D., Petrillo, Z., Rodrigues, T., Voelker, A.H., Amore, F.O., 2013b. Abrupt variability of the last 24 ka BP recorded by coccolithophore assemblages off the Iberian margin (core MD03-2699). J. Quat. Sci. 28 (3), 320–328.
Parente, A., Cachão, M., Baumann, K.H., de Abreu, L., Ferreira, J., 2004. Morphometry of Coccolithus pelagicus sl (Coccolithophore, Haptophyta) from offshore Portugal, during the last 200 kyr. Micropaleontology 50 (Suppl_1), 107–120.
Peliz, Á., Dubert, J., Haidvogel, D.B., Le Cann, B., 2003. Generation and unstable evolution of a density-driven eastern poleward current: the Iberian poleward current. J. Geophys. Res. Oceans 108 (38), 3268. https://doi.org/10.1029/2002JC001443.
Peliz, A., Dubert, J., Santos, A., Oliveira, P., Le Cann, B., 2005. Winter upper ocean circulation in the Western Iberian Basin—Fronts, eddies and poleward flows: An overview, Deep Sea Res. Part I 52, 621–646.
Peliz, A., Dubert, J., Marchesiello, P., Teles-Machado, A., 2007. Circulation in the Gulf of Cadiz: Model and mean flow structure. J. Geophys. Res. 112, C11015. https://doi.org/10.1029/2007JC004159.
Pénaud, A., Eynaud, F., Sánchez-Goñi, M., Malaizé, B., Turon, J.L., Rossignol, L., 2011. Contrasting Sea-surface responses between the western Mediterranean Sea and eastern subtropical latitudes of the North Atlantic during abrupt climatic events of MIS 3. Mar. Micropaleontol. 80 (1–2), 1–17.
Penaud, A., Eynaud, F., Voelker, A.H.L., Turon, J.L., 2016. Palaeohydrological changes over the last 50 ky in the central Gulf of Cadiz: complex forcing mechanisms mixing multi-scale processes. Biogeosciences 13 (18), 5357–5377.
Penaud, A., Eynaud, F., Etourneau, J., Bonnin, J., de Vernal, A., Zaragosi, S., Kim, J.H., Kang, S., Gal, J.K., Oliveira, D., Waelbroeck, C., 2022. Ocean productivity in the Gulf of Cadiz over the last 50 kyr. Paleoceanograph. Paleoclimatol. 37 (2). https://doi.org/10.1029/2021PA004316.
Pérez, F.F., Castro, C.G., Álvarez–Salgado, X.A., Ríos, A.F. 2001. Coupling between the Iberian basin—scale circulation and the Portugal boundary current system: a chemical study. Deep-Sea Res. I Oceanogr. Res. Pap. 48(6), 1519–1533.
Pittalwala, I., Hameed, I., 1991. Simulation of the North Atlantic Oscillation in a general circulation model. Geophys. Res. Lett. 18, 841–844.
Prahl, F., Wakeham, S., 1987. Calibration of unsaturation patterns in long-chain ketone compositions for palaeotemperature assessment. Nature 330, 367–369. https://doi.org/10.1038/330367a0.
Quivelli, O., Marino, M., Rodrigues, T., Girone, A., Maiorano, P., Abrantes, F., Salgueiro, E., Bassinot, F., 2020. Surface and deep water variability in the Western Mediterranean (ODP Site 975) during insolation cycle 74: High-resolution calcareous plankton and molecular biomarker signals. Palaeogeogr. Palaeoclimatol. Palaeoecol. 542, 109583. https://doi.org/10.1016/j.palaeo.2019.109583.
Quivelli, O., Marino, M., Rodrigues, T., Girone, A., Maiorano, P., Bertini, A., Niccolini, G., Trotta, S., Bassinot, F., 2021. Multiproxy record of suborbital-scale climate changes in the Algero-Balearic Basin during late MIS 20 - termination IX. Quat. Sci. Rev. 260, 106916. https://doi.org/10.1016/j.quascirev.2021.106916.
Rahmstorf, S., 2002. Ocean circulation and climate during the past 120,000 years. Nature 419 (6903), 207–214. https://doi.org/10.1038/nature01090 (PMID: 12226675).
Raymo, M.E., Nisancioglu, K.H., 2003. The 41 kyr world: Milankovitch's other unsolved mystery. Paleoceanography 18, 11–16.
Raymo, M.E., Ganley, K., Carter, S., Oppo, D.W., McManus, J., 1998. Millennial-scale climate instability during the early Pleistocene epoch. Nature 392 (6677), 699–702. https://doi.org/10.1038/33658.
Reagan, J.R., Boyer, T.P., Garcia, H.E., Locarnini, R.A., Baranova, O.K., Bouchard, C., Cross, S.L., Mishonov, A.V., Paver, C.R., Seidov, D., Wang, Z., Dukhovskoy, D., 2024. World Ocean Atlas 2023, NCEI Accession 0270533, NOAA National Centers for Environmental Information (Dataset).
Rodó, X., Baert, E., Comin, F.A., 1997. Variations in seasonal rainfall in Southern Europe during the present century: relationships with the North Atlantic Oscillation and the El Niño-Southern Oscillation. Clim. Dyn. 13, 275–284.
Rodrigues, T., Grimalt, J.O., Abrantes, F.G., Flores, J.A., Lebreiro, S.M., 2009. Holocene interdependences of changes in sea surface temperature, productivity, and fluvial inputs in the Iberian continental shelf (Tagus mud patch). Geochem. Geophys. Geosyst. 10, Q07U06. https://doi.org/10.1029/2008GC002367.

Rodrigues, T., Voelker, A.H.L., Grimalt, J.O., Abrantes, F., Naughton, F., 2011. Iberian margin sea surface temperature during MIS 15 to 9 (580-300 ka): glacial suborbital variability versus interglacial stability. Paleoceanography 26 (1), PA1204. https://doi.org/10.1029/2010PA001927.

Rodrigues, T., Alonso-García, M., Hodell, D.A., Rufino, M., Naughton, F., Grimalt, J.O., Voelker, A.H.L., Abrantes, F., 2017. A 1-Ma record of sea surface temperature and extreme cooling events in the North Atlantic: a perspective from the Iberian margin. Quat. Sci. Rev. 172, 118–130. https://doi.org/10.1016/j.quascirev.2017.07.004.

Rohling, E.J., Foster, G.L., Grant, K.M., Marino, G., Roberts, A.P., Tamisiea, M.E., Williams, F., 2014. Sea-level and deep-sea-temperature variability over the past 5.3 million years. Nature 508, 477–482.

Saavedra-Pellitero, M., Flores, J.A., Baumann, K.H., Sierro, F.J., 2010. Coccolith distribution patterns in surface sediments of Equatorial and Southeastern Pacific Ocean. Geobios 43 (1), 131–149.

Schulz, M., 2002. On the 1470-year pacing of Dansgaard-Oeschger warm events. Paleoceanography 17 (2), 4–1.

Sepulcre, S., Vidal, L., Tachikawa, K., Rostek, F., Bard, E., 2011. Sea-surface salinity variations in the northern Caribbean Sea across the Mid-Pleistocene transition. Clim. Past 7 (1), 75–90.

Serrano, F., Guerra-Merchán, A., 2012. Sea-surface temperature for left-coiling Neogloboquadrina populations inhabiting the westernmost Mediterranean in the middle Pleistocene and the Pleistocene-Pliocene transition. Geobios 45, 231–240. https://doi.org/10.1016/j.geobios.2011.04.003.

Shackleton, N.J., Hall, M.A., Vincent, E., 2000. Phase relationships between millennial-scale events 64,000–24,000 years ago. Paleoceanography 15 (6), 565–569.

Shackleton, N., Fairbanks, R., Chien Chiu, T., Parrenin, F., 2004. Absolute calibration of the Greenland time scale: implications for Antarctic time scales and for ^{14}C. Quat. Sci. Rev. 23, 1513–1522. https://doi.org/10.1016/j.quascirev.2004.03.006.

Siddall, M., Rohling, E.J., Thompson, W.G., Waelbroeck, C., 2008. Marine isotope stage 3 sea level fluctuations: Data synthesis and new outlook. Rev. Geophys. 46, RG4003. https://doi.org/10.1029/2007RG000226.

Stein, R., Hefter, J., Grützner, J., Voelker, A., Naafs, B.D.A., 2009. Variability of surface water characteristics and Heinrich-like events in the Pleistocene mid latitude North Atlantic Ocean: biomarker and XRD records from IODP site U1313 (MIS 16e9). Paleoceanography 24, PA2203. https://doi.org/10.1029/2008PA001639.

Steinmetz, J.C., 1991. Calcareous nannoplankton biocoenosis: sediment trap studies in the Equatorial Atlantic, Central Pacific, and Panama Basin. Woods Hole Oceanographic Institution. Report 1, 1–85.

Stoll, H.M., Arevalos, A., Burke, A., Ziveri, P., Mortyn, G., Shimizu, N., Unger, D., 2007. Seasonal cycles in biogenic production and export in Northern Bay of Bengal sediment traps. Deep-Sea Res. II Top. Stud. Oceanogr. 54 (5–7), 558–580.

Sun, Y., McManus, J.F., Clemens, S.C., Zhang, X., Vogel, H., Hodell, D.A., Guo, F., Wang, T., Liu, X., An, Z., 2021. Persistent orbital influence on millennial climate variability through the Pleistocene. Nat. Geosci. 14 (11), 812–818. https://doi.org/10.1038/s41561-021-00794-1.

Teles-Machado, A., Peliz, A., McWilliams, J.C., Couvelard, X., Ambar, I., 2016. Circulation on the Northwestern Iberian margin: Vertical structure and seasonality of the alongshore flows. Prog. Oceanogr. 140, 134–153. https://doi.org/10.1016/j.pocean.2015. 05.021.

Torrence, C., Compo, G.C., 1998. A practical guide to wavelet analysis. Bull. Am. Meteorol. Soc. 79, 61–78.

Trigo, R.M., Osborn, T.J., Corte-Real, J.M., 2002. The North Atlantic Oscillation influence on Europe: climate impacts and associated physical mechanisms. Clim. Res. 20 (1), 9–17.

Trigo, R.M., Pozo-Vázquez, D., Osborn, T.J., Castro-Díez, Y., Gámiz-Fortis, S., Esteban-Parra, M.J., 2004. North Atlantic Oscillation influence on precipitation, river flow and water resources in the Iberian Peninsula. Int. J. Climatol. 24 (8), 925–944.

Trommer, G., Siccha, M., Rohling, E.J., Grant, K., van der Meer, M.T.J., Schouten, S., Baranowski, U., Kucera, M., 2011. Sensitivity of Red Sea circulation to sea level and insolation forcing during the last interglacial. Clim. Past Discuss. 7, 119–1233.

Trotta, S., Marino, M., Maiorano, P., Girone, A., 2019. Climate variability through MIS 20-MIS 19 in core KC01B, Ionian Basin (Central Mediterranean Sea). Alpine Mediterranean Quatern. 32 (2), 151–165.

Trotta, S., Marino, M., Voelker, A.H.L., Rodrigues, T., Maiorano, P., Flores, J.A., Girone, A., Addante, M., Balestra, B., 2022. Paleoenvironmental reconstruction in the Gulf of Cadiz using calcareous nannofossil assemblages during the early Pleistocene (MIS 48-MIS 45). Palaeogeogr. Palaeoclimatol. Palaeoecol. 608, 111304.

Trotta, S., Marino, M., Maiorano, P., Voelker, A.H.L., 2024. Coccolithophore paleoproductivity reveals past oceanographic and atmospheric climate dynamics. Past Global Changes Magazine 32 (2), 108–109. https://doi.org/10.22498/pages.32.2.108.

Tzedakis, P.C., 2010. The MIS 11–MIS 1 analogy, southern European vegetation, atmospheric methane and the“ early anthropogenic hypothesis”. Clim. Past 6 (2), 131–144.

Tzedakis, P.C., Margari, V., Hodell, D.A., 2015. Coupled ocean-land millennial scale changes 1.26 million years ago, recorded at Site U1385 off Portugal. Glob. Planet. Chang. 135, 83–88. https://doi.org/10.1016/j.gloplacha.2015.10.008.

van Aken, H.M., 2001. The hydrography of the mid-latitude Northeast Atlantic Ocean – Part1046 III: the subducted thermocline water mass. Deep-Sea Res. I Oceanogr. Res. Pap. 48 (1), 237–267.

Villanueva, J., Pelejero, C., Grimalt, J.O., 1997. Clean-up procedures for the unbiased estimation of C37 alkenone sea surface temperatures and terrigenous n-alkane inputs in paleoceanography. J. Chromatogr. A 757 (1–2), 145–151.

Voelker Antje, H.L., Rodrigues, T., Trotta, S., Marino, M., Kuhnert, H., 2022. Isotope ratios of foraminifera of IODP Site 339-U1387. PANGAEA. https://doi.org/10.1594/PANGAEA.951453.

Voelker, A.H.L., et al., 2002. Global distribution of centennial-scale records for marine isotope stage (MIS) 3: a database. Quat. Sci. Rev. 21, 1185–1214.

Voelker, A.H.L., Salgueiro, E., Rodrigues, T., Jimenez-Espejo, F.J., Bahr, A., Alberto, A., Loureiro, I., Padilha, M., Rebotim, A., Röhl, U., 2015. Mediterranean Outflow and surface water variability off southern Portugal during the early Pleistocene: A snapshot at Marine Isotope Stages 29 to 34 (1020–1135 ka). Glob. Planet. Chang. 133, 223–237. https://doi.org/10.1016/j.gloplacha.2015.08.015.

Voelker, A.H.L., Jimenez-Espejo, F.J., Bahr, A., Rebotim, A., Cavaleiro, C., Salgueiro, E., Röhl, U., 2018. Data report: IODP Site U1387: the revised splice between Sections U1387B-18X-3 and U1387C-8R-3 (>171.6 mcd). In: Stow, D.A.V., Hernández-Molina, F.J., Alvarez Zarikian, C.A. (Eds.), Expedition 339 scientists, Proceedings of the Integrated Ocean Drilling Program, 339: Tokyo (Integrated Ocean Drilling Program Management International, Inc.). https://doi.org/10.2204/iodp.proc.339.204.2018.

Voelker, A.H., Rodrigues, T., Trotta, S., Marino, M., Kuhnert, H., 2022a. A southern Portuguese margin perspective of Marine Isotope Stage 47—An interglacial in the 41 kyr World. Atmosphere 13 (9), 1378. https://doi.org/10.3390/atmos13091378.

Voelker, A.H.L., Rodrigues, T., Trotta, S., Marino, M., Kuhnert, H., 2022c. Sea surface temperature reconstruction based on UK37 for IODP Site 339-U1387. PANGAEA. https://doi.org/10.1594/PANGAEA.951451.

Winter, A., Siesser, W.G., 1994. Coccolithophores, 42pp. Cambridge University Press, New York.

Young, J.R., Geisen, M., Cros, L., Kleijne, A., Sprengel, C., Probert, I., Østergaard, J., 2003. A guide to extant coccolithophore taxonomy. J. Nannoplankton Res. Spe. Issue 1–132.

Young, J.R., Bown, P.R., Lees, J.A., 2022. Nannotax3 Website. International Nannoplankton Association. Accessed 21 Apr. 2022. URL. www.mikrotax.org/Nannotax3.

Zamelczyk, K., Fransson, A., Chierici, M., Jones, E., Meilland, J., Anglada-Ortiz, G., Lødemel, H.H., 2021. Distribution and abundances of planktic foraminifera and shelled Pteropods during the polar night in the sea-ice covered northern Barents Sea. Front. Mar. Sci. 8, 644094. https://doi.org/10.3389/fmars.2021.644094.

Zhang, X., Barker, S., Knorr, G., Lohmann, G., Drysdale, R., Sun, Y., Hodell, D., Chen, F., 2021. Direct astronomical influence on abrupt climate variability. Nat. Geosci. 14 (11), 819–826. https://doi.org/10.1038/s41561-021-00846-6.

Ziegler, M., Nürnberg, D., Karas, C., Tiedemann, R., Lourens, L.J., 2008. Persistent summer expansion of the Atlantic warm Pool during glacial abrupt cold events. Nat. Geosci. 1 (9), 601–605.

Ziveri, P., Thunell, R.C., Rio, D., 1995. Seasonal changes in coccolithophore densities in the Southern California Bight during 1991–1992. Deep-Sea Res. I Oceanogr. Res. Pap. 42 (11−12), 1881–1903.

Ziveri, P., Baumann, K.H., Böckel, B., Bollmann, J., Young, J.R., 2004. Biogeography of Selected Holocene Coccoliths in the Atlantic Ocean. From Molecular processes to global impact, Coccolithophores, pp. 403–428.